MEASUREMENT AND ANALYSIS OF AIRCRAFT FAR-FIELD AERODYNAMIC NOISE

Gerald J. Healy

1. Report No. NASA CR-2377	2. Government Accession No.	3. Recipient's Catalog No.
4. Title and Subtitle Measurement and Analysis of Aircraft Far-Field Aerodynamic Noise		5. Report Date December 1974
		6. Performing Organization Code
7. Author(s) Gerald J. Healy		8. Performing Organization Report No. LR 26195
		10. Work Unit No.
9. Performing Organization Name and Address Lockheed-California Company P. O. Box 551 Burbank, Ca. 91520		
		11. Contract or Grant No. NAS 1-12440
		13. Type of Report and Period Covered Contractor Report
12. Sponsoring Agency Name and Address National Aeronautics and Space Administration Washington, D. C. 20546		
		14. Sponsoring Agency Code

15. Supplementary Notes

Final report.

16. Abstract

The work reported herein is the first systematic investigation of aircraft far-field radiated, aerodynamically generated noise. The test phase of the original program involved the measurement of the noise produced by five gliding aircraft in an aerodynamically "clean" configuration during low altitude flyovers. These aircraft had gross weights that ranged from 5785 to 173 925N (1300 to 39 000 pounds), fly-by velocities from 30 to 98.5 m/sec (58 to 191.5 knots or 98 to 323 ft/sec) and wing aspect ratios from 6.59 to 18.25. The results of these measurements were used to develop an equation relating aerodynamic noise to readily evaluated physical and operational parameters of the aircraft. A non-dimensional frequency spectrum, based on the mean wing thickness, was also developed.

17. Key Words (Suggested by Author(s)) Noise; Airframe Noise; Far-field Aerodynamic Noise	18. Distribution Statement Unclassified-unlimited STAR Category 02		
19. Security Classif. (of this report) Unclassified	20. Security Classif. (of this page) Unclassified	21. No. of Pages 69	22. Price* $4.25

CONTENTS

LIST OF ILLUSTRATIONS

LIST OF TABLES

NOMENCLATURE

$AR = b^2/S$ — aspect ratio

b — wing span, m (ft)

c — wing chord, m (ft)

c_1, c_2, c_3 — mean wing chord (see text for definitions), m (ft)

$C_L = \dfrac{L}{\dfrac{\rho}{2}V^2 S}$ — lift coefficient

f — frequency, Hz

$F(\ )$ — function relating aircraft parameters to dipole strength

K — constant of proportionality

L — lift, N (lb)

M — Mach number

n — test run number

$OASPL$ — overall sound pressure level, dB re 2×10^{-5} N/sq m

r — range from aircraft to observer, m (ft)

S — wing area, sq m (sq ft)

SPL — sound pressure level, dB re 2×10^{-5} N/sq m

S_t — Strouhal number

t — wing thickness, m (ft)

t_1, t_2, t_3 — mean wing thickness (see text for definitions), m (ft)

V — velocity, m/sec (knots or ft/sec)

W — weight, N (lb)

W/b — span loading, N/m(lb/ft)

W/S — wing loading, N/sq m (lb/sq ft)

$X1, X2, X3, X4, X5, X6, X7$ — arbitrary exponents for terms in $F(\ )$

ϕ — elevation angle of aircraft

MEASUREMENT AND ANALYSIS OF AIRCRAFT
FAR-FIELD AERODYNAMIC NOISE

By Gerald J. Healy
Lockheed-California Company

SUMMARY

The work reported herein – the first systematic investigation of far-field radiated, aerodynamically generated noise – involved the measurement of the noise produced by five gliding aircraft in a "clean" configuration during low altitude flyovers. These aircraft had gross weights that ranged from 5785 to 173 925 N (1300 to 39 000 pounds), fly-by velocities from 30 to 98.5 m/sec (58 to 191.5 knots or 98 to 323 ft/sec) and wing aspect ratios from 6.59 to 18.25. The results of these measurements were used to develop an equation relating aerodynamic noise to readily evaluated physical and operational parameters of the aircraft.

Using the resulting prediction method, it is now possible to calculate, with a reasonable level of confidence, the overall sound pressure level and to estimate the frequency distribution of the far-field radiated, aerodynamically generated noise of "clean" configured aircraft in flight. Knowledge of the aerodynamic noise "floor" established by such aircraft sets limits for effective power-plant noise reduction. Additionally, insight is provided for both quieting existing aircraft and designing new aircraft to be aerodynamically quiet.

INTRODUCTION

Recently, the need to predict the minimum noise produced by an aircraft, i.e., the non-propulsive noise resulting from the motion of the aircraft through the air (ref. 1, 2, 3 and 4), has been stimulated by the desire, on the part of the aircraft industry, to design commercial transports with reduced community noise levels. The Lockheed-California Company (Calac) became keenly interested in this source of flyover noise in 1969 when the company was under contract with the Naval Air Systems Command (NASC), Washington, D. C., to study the design of quiet reconnaissance aircraft. While reasonably accurate estimations could be made of the noise produced by the acoustically quieted propulsion systems under consideration, the far-field noise produced by the motion of the airframe through the air eluded accurate prediction. This void in the far-field noise signature of the aircraft under consideration seriously impacted evaluation of the vehicle aural detection distance. Consequently, an experimental program encompassing the measurement of the far-field radiated aerodynamically generated noise was developed and proposed to the NASC.

Because of the fundamental and general nature of the proposed program, the National Aeronautics and Space Administration (NASA) was also approached. The result was a two-phase program of which the first phase, funded by Calac, involved the testing of a company-owned Douglas DC-3 (ref. 5). The purpose of this initiatory program was to determine whether or not the far-field aerodynamic noise was measurable and, if so, then

to develop the flight testing procedures and establish data acquisition instrumentation requirements and data reduction methodology prior to the commencement of phase two. The second phase, jointly funded by the NASC and the NASA, encompassed the testing of two additional two-engine aircraft (Convair 240 and Aero-Commander Shrike) and a glider. During the phase two flight test program, limited data were also acquired on a single-engine Cessna 150. Propeller driven aircraft were selected because the acoustical contribution of the propulsion system could be virtually eliminated by stopping the engines and feathering the propellers (bringing the propellers to a standstill) during noise measurements and then re-starting the engines following the completion of the fly-over.

Because the measurement program was scheduled to dovetail with the aforementioned quiet reconnaissance aircraft study program, the data analysis was, of necessity, directed toward rapidly isolating the most influential variables and developing a suitable prediction method for application to that program. These rather limited objectives were fulfilled, the study being completed in June 1970 (ref. 13 of ref. 1).

The prediction methodology was then applied to a number of other aircraft ranging form a variety of reconnaissance aircraft to large commercial transports. However, since the original analysis was directed toward aircraft having gross weights under 178 000 N (40 000 lb), the extrapolation of these data to substantially larger aircraft carried with it an element of uncertainty. Recognition of this problem, and the need to resolve it, as well as the desire to make these original data more readily available, provided the impetus for the present study.

The primary objective of this follow-on study, therefore, was to re-analyze the original data by applying the experience gained subsequent to the completion of that study, in order to improve the prediction methodology for aerodynamically "clean" aircraft. This objective was realized and produced a substantial improvement in the correlation between the measured and predicted overall sound pressure levels. In addition, the improved prediction technique has been applied to recently acquired data on a "clean" configured C-5A (refs. 3 and 4) and has demonstrated excellent agreement between the measured and predicted noise levels. These promising results have fulfilled a secondary objective -- that of removing the uncertainty associated with extrapolation of these data to large aircraft.

The successful development of an accurate far-field aerodynamic noise prediction method for "clean" configured aircraft:

- Establishes the limits for effective transport aircraft engine noise reduction

- Provides design guidance for minimizing aircraft aerodynamic noise

- Permits estimation of the contribution of operational variables to the aerodynamically generated noise

- Permits computation of the aerodynamic noise associated with existing aircraft

- Provides a method for evaluating the impact of design and/or operational changes to existing aircraft on this noise source.

These important benefits to the field of aircraft noise prediction, while a direct outgrowth of a military sponsored quiet reconnaissance aircraft study program, will have their greatest application to commercial transport aircraft since the ability to predict the noise "floor" of an aircraft is of major importance to both manufacturer and Federal regulatory agencies.

The present report, prepared under contract NAS1-12440 with the National Aeronautics and Space Administration, Langley Research Center, Hampton, Virginia, is based on work performed under both a company-funded Independent Research program (ref. 5) and under Contract Number N00123-70-C-0906 for the U. S. Naval Air Systems Command, Washington, D. C. (ref. 13 or ref. 1). The latter program was jointly funded by the U. S. Naval Air Systems Command and the National Aeronautics and Space Administration.

PROGRAM SCOPE

The objective of the study reported here is to develop a theory-based empirical equation containing the pertinent vehicle and environmental parameters for the prediction of the far-field radiated aerodynamic noise from an aerodynamically "clean" aircraft. Aerodynamically "clean" means a low drag airframe with no sharp surface discontinuities or protrusions that would be prone to the generation of very narrow bands of random noise which approach pure tone characteristics. Aerodynamic noise was measured under controlled conditions for a number of aircraft. As part of the analysis, the associated frequency spectra were "smoothed" to remove the effects of any "pure tones" associated with the particular aircraft as a result of such protrusions as antennas, pitot tubes, etc. The resulting overall sound pressure level values were then used to evaluate the exponents of some important aircraft parameters in a generalized equation for the radiated aerodynamic noise. To complete the study the associated frequency spectrum, expressed as a non-dimensional frequency based on a typical vehicle dimension, viz. mean wing thickness, was also developed.

The total program covered a broad spectrum of relatively small aircraft:

- Heavy Twin, 164 585 N (37 000 pound) class (Convair 240)

- Medium Twin, 102 310 N (23 000 pound) class (Douglas DC-3)

- Light Twin, 26 690 N (6000 pound) class (Aero-Commander Shrike)

- Glider, 6670 N (1500 pound) class (Prue-2)

- Light Single, 6670 N (1500 pound) class (Cessna 150)

Figures 1 through 5 present three-view drawings of these aircraft obtained from references 6 through 9. All aircraft, with the exception of the Cessna 150, were flown at three or four different velocities and two different gross weights. The Cessna was flown at one gross weight and two velocities. Table I summarizes pertinent dimensional data on these aircraft.
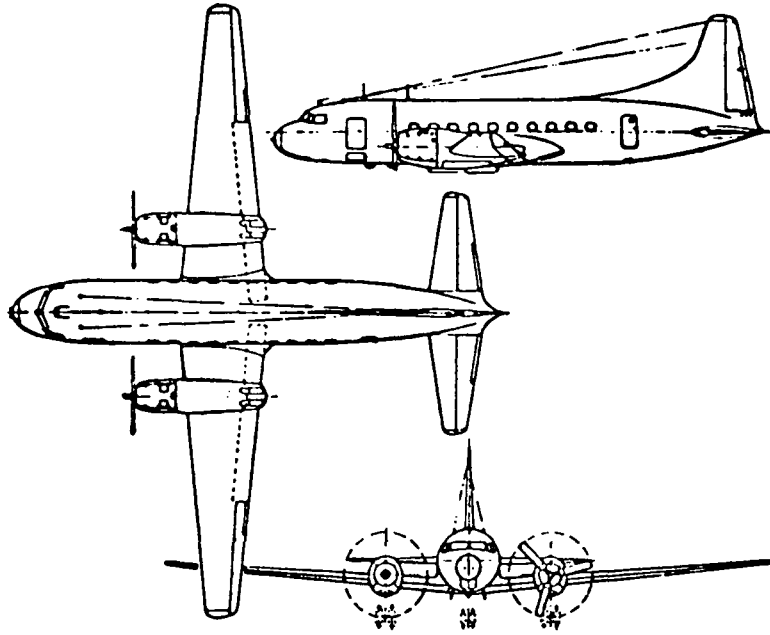
Figure 1. – Convair 240
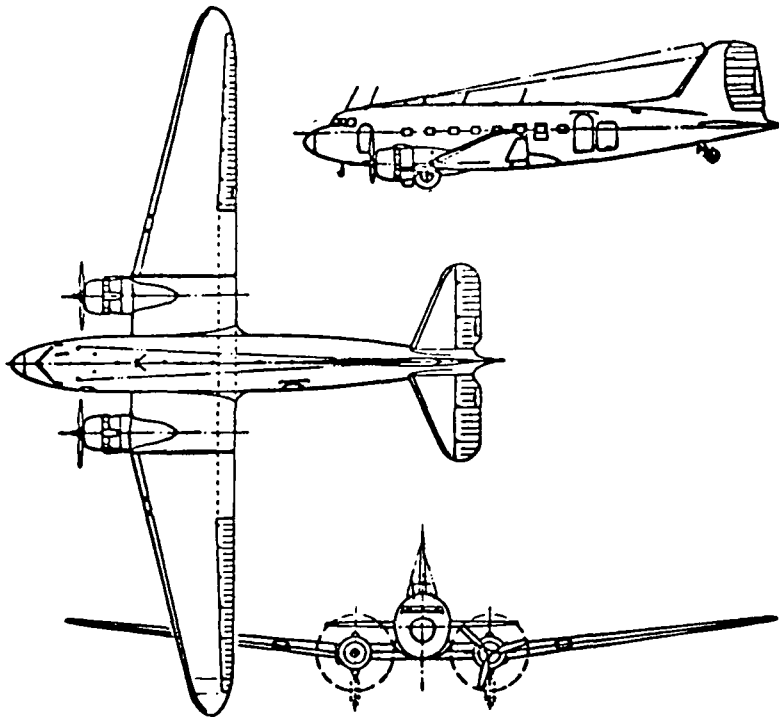
Figure 2. – Douglas DC-3
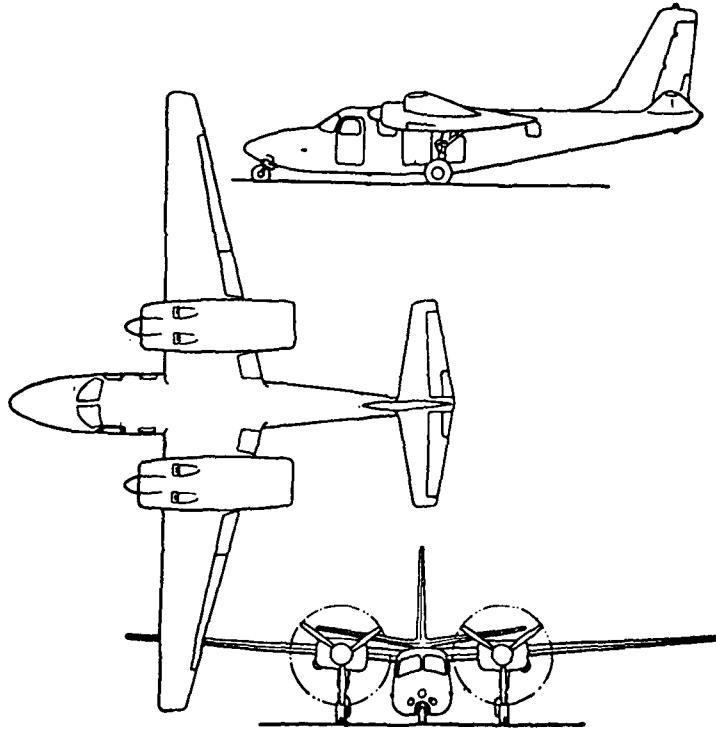
Figure 3. – Aero-Commander Shrike
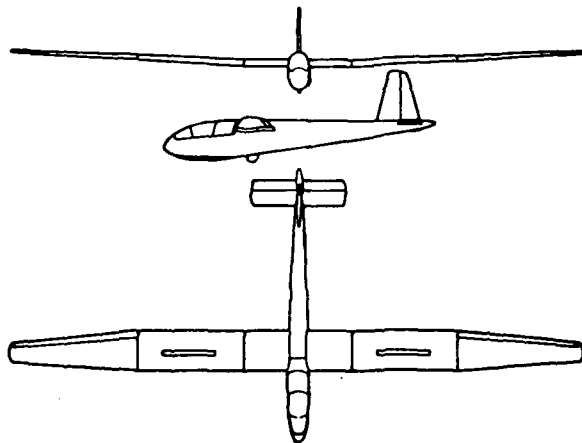
Figure 4. – Prue-2
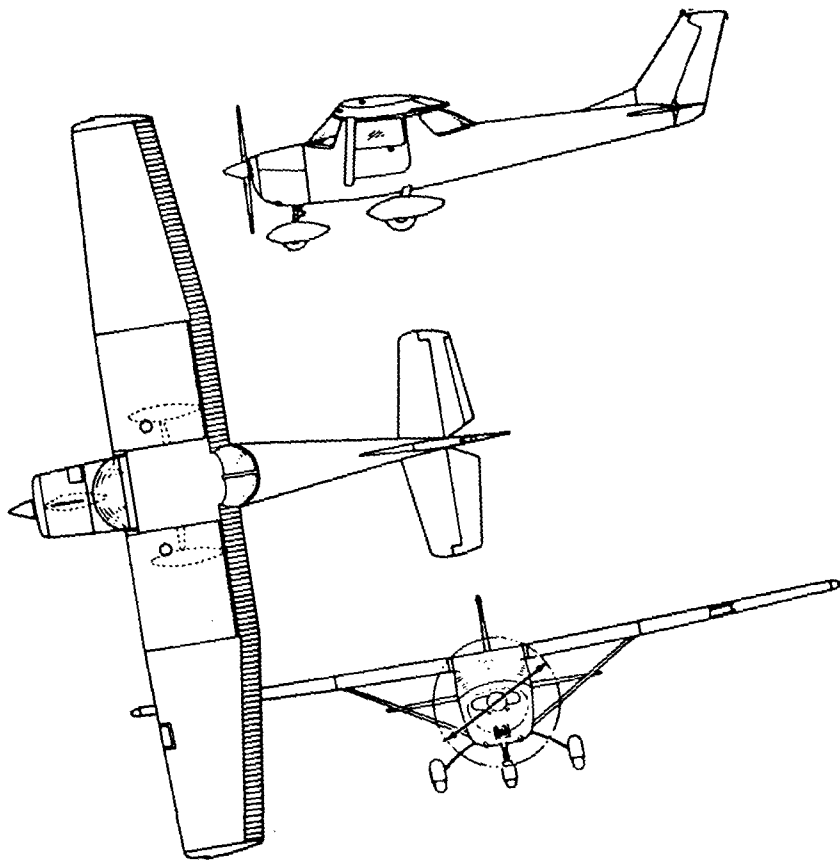
Figure 5. – Cessna 150

TABLE I

AIRCRAFT DATA

Aircraft Parameters	Convair 240	Douglas DC-3	Aero-Commander Shrike	Prue-2 (Glider)	Cessna 150
Weight, N (lb) Min	153 465 (34 500)	100 085 (22 500)	22 685 (5100)	5785 (1300)	6895 (1550)
Max	173 925 (39 100)	112 095 (25 200)	29 135 (6550)	7120 (1600)	—
Mass, kg Min	15 650	10 205	2315	590	705
Max	17 735	11 430	2970	725	—
Wing Area, m^2 (ft^2)	75.9 (817)	91.7 (987)	23.7 (255)	21.2 (228)	14.6 (157)
Wing Span, m (ft)	27.97 (91.75)	28.96 (95.0)	14.95 (49.04)	19.66 (64.5)	9.97 (32.71)
Aspect Ratio	10.3	9.14	9.43	18.25	6.59
Avg Chord*, m (ft): C_1	2.85 (9.34)	3.57 (11.70)	1.75 (5.75)	N.A.	N.A.
C_2	2.58 (8.46)	3.07 (10.07)	1.50 (4.93)		
C_3	2.71 (8.90)	3.17 (10.39)	1.58 (5.20)		
Avg Thickness*, m (ft): t_1	.54 (1.77)	.49 (1.62)	.21 (.69)	N.A.	N.A.
t_2	.48 (1.57)	.39 (1.26)	.18 (.59)		
t_3	.51 (1.67)	.41 (1.33)	.19 (.62)		

*See Text for Definitions
N.A. – Not Analyzed (See Text)

8

DATA ACQUISITION AND REDUCTION PROCEDURES

Test Program

Most of the flight tests for the measurement of aerodynamic noise were performed at El Mirage Dry Lake, California. This test location provided low ambient noise levels and space for landing, if required, after the "dead stick" (unpowered) flyovers. Because of rain water standing in the El Mirage lake bed, the last test series on the glider was performed at the Helendale, California, airstrip. For all tests, air temperature ranged from 280° to 300°K (44° to 80°F), and the relative humidity was from 30 to 69 percent. Wind speeds were, in general, under 2.6 meters per second (5 knots). The initial tests (on the DC-3) were made on 1 August 1969 and the last tests (on the glider) were made on 12 March 1970.

The flight tests were performed in the following manner. The instrumentation was set up prior to sunrise in order to complete the day's data acquisition before the desert winds began. The self-powered aircraft were flown to an altitude of approximately 610 meters (2000 feet) from which the descent was initiated. Except for the Cessna, the engines were shut down, the propellers feathered (stationary attitude), the wheels kept retracted, and the flaps in the normal cruise position, thereby making the aircraft as aerodynamically "clean" as possible. A typical flight profile is presented in figure 6. All aspects of the Cessna tests were the same as those for the two-engine aircraft except that the Cessna did not have a retracting gear, and this particular aircraft did not have wheel fairings. The fixed pitch propeller of the Cessna windmilled during the high speed run, but stopped completely during the low speed run. The Prue-2 glider was towed to a convenient "holding" altitude until conditions were all right for a test run, at which time the pilot made the test pass and then landed. For several runs the pilot made the high speed run at a "high" altitude, turned around, and made the low speed run at a "low" altitude before landing.

The aircraft were flown at a nominal altitude of 152.4 meters (500 feet) over the measurement microphones. This relatively low altitude was selected to provide a high ratio of signal (aerodynamic noise) to ambient noise. Aircraft altitudes were determined by photographing each flyover with a Polaroid camera whose image size factor was known. The actual altitude was computed by using the image size factor and a known aircraft dimension. In this case the aircraft wingspan served as the reference dimension. The photograph was taken at the moment the aircraft was directly overhead. Simultaneously, a verbal statement was placed on the voice channel in order to provide a reference, during data reduction, between aircraft position and noise level. Except for the glider tests, actual altitudes ranged from 97.5 to 241 meters (320 to 790 feet). The glider tests were made in two series -- the first series was flown at the nominal altitude of 152.4 meters (500 feet), but the signal level of the aerodynamic noise was too low to be separated from the ambient noise. The second series of tests was flown at altitudes that ranged from 46 to 109 meters (152 to 357 feet) and produced measurable data.

Three nominal aircraft speeds were selected for each aircraft to cover a wide but operationally safe speed range. The total speed range, including all aircraft, was from about 30 to 98.5 meters per second (58 to 191.5 knots). Runs were repeated if the actual speeds or altitudes were judged to be too far from the preselected nominal values or if

ENGINE
POWER OFF –
PROPELLERS
FEATHERED

ACCELERATION
TO TEST VELOCITY

DESCENT AT
CONSTANT
FORWARD
VELOCITY

BEGIN RETURN
FLIGHT FOR
NEXT TEST
CONDITION

ENGINE
START-UP

GROUND
STATION

(NOT TO SCALE)
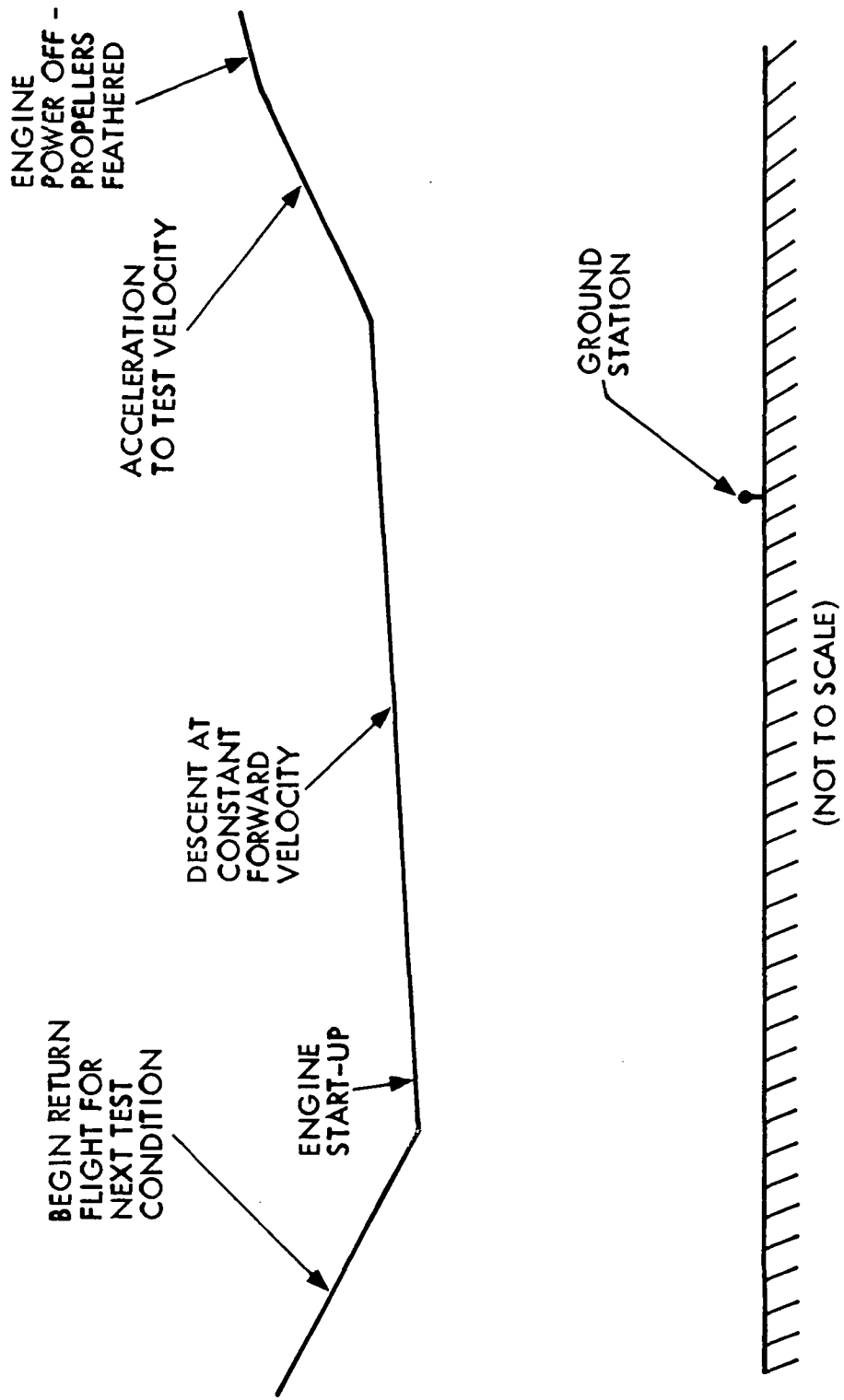
Figure 6. Typical Flight Profile

high ambient noise from nearby aircraft was detected during the test run. Aircraft speed was determined by pilot readings of the airspeed indicator; average values of the pilot and copilot meter readings were used for the Convair and DC-3 flyovers. The accuracy of the calculated true airspeeds is approximately plus or minus one meter per second (± 2 knots).

During the flyovers, noise was measured with two capacitance type microphones, with windscreens, located on a line perpendicular to the flight path at positions 30.5 meters (100 feet) to either side of the target point over which the airplane flew as shown below:

```
                                          ↑
                                              ╱─BASE STATION
                                          │  ╱
                                          │ ╱
   SOUTH          30.5 m              ┌──┼─┐         30.5 m          NORTH
     ○────────────────────────────────│──✕─│────────────────────────────────○
   MICROPHONE     (100 ft)            └──┼──┘         (100 ft)      MICROPHONE
                                          │
                                          │
                                          │
                                          │
                                       AIRCRAFT
                                       FLIGHT
                                       PATH
```
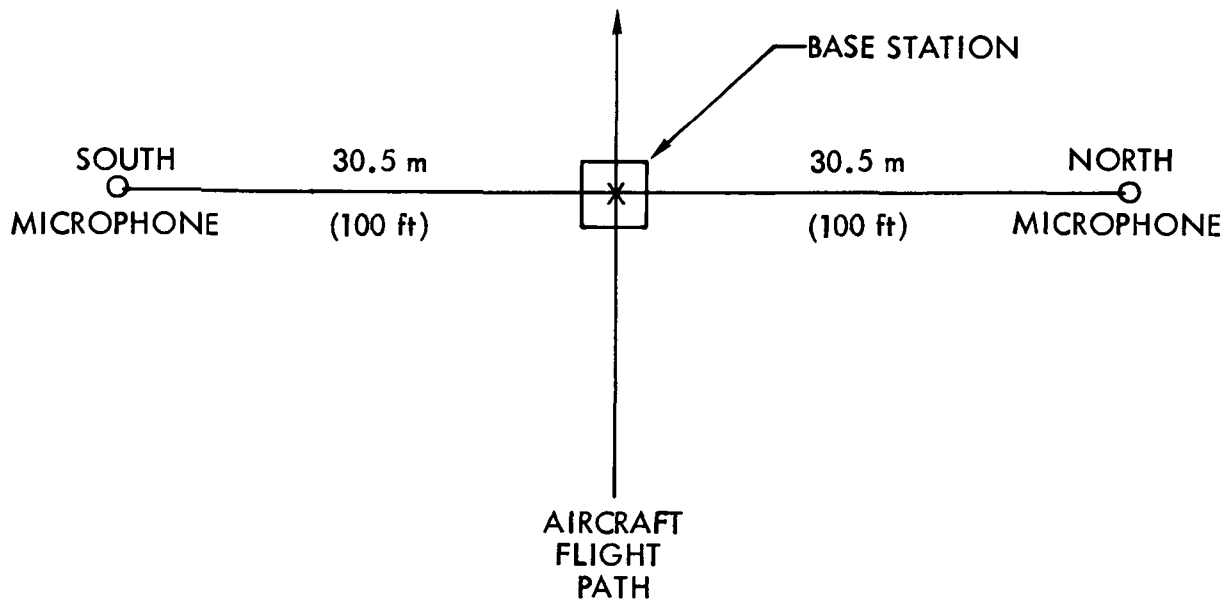
These microphones were field calibrated prior to and after each day's tests -- a time span of from two to four hours. The ground station and recording equipment are shown in figure 7, photographed during a low altitude practice flyover of the Convair 240. The microphone outputs were FM recorded on a wideband 14-channel magnetic tape recorder.

A verbal description and identification of each test or calibration was recorded on a separate voice channel. This channel was also used to note the time the aircraft was directly overhead. The acquisition equipment was operated for about one minute before and after each flyover. Typical ambient noise records were made several times throughout each day's tests.

In addition to the data being recorded on magnetic tape, an on-site sound level meter was used to confirm the tape recorded data. The peak reading of the sound level meter was noted and manually recorded on the test data sheets during each flyover. Wind speed and direction readings were made during the flyover, and air temperature readings were made within one minute after each flyover. Wet and dry bulb thermometer readings were taken at the start and end of each day's testing.

All measurements were made using the English system of units.

Figure 7. – Practice Test at El Mirage Dry Lake, California

Instrumentation

The data acquisition equipment was set up at the east end of El Mirage Dry Lake as shown in the previous section. Electrical power for the base station equipment was provi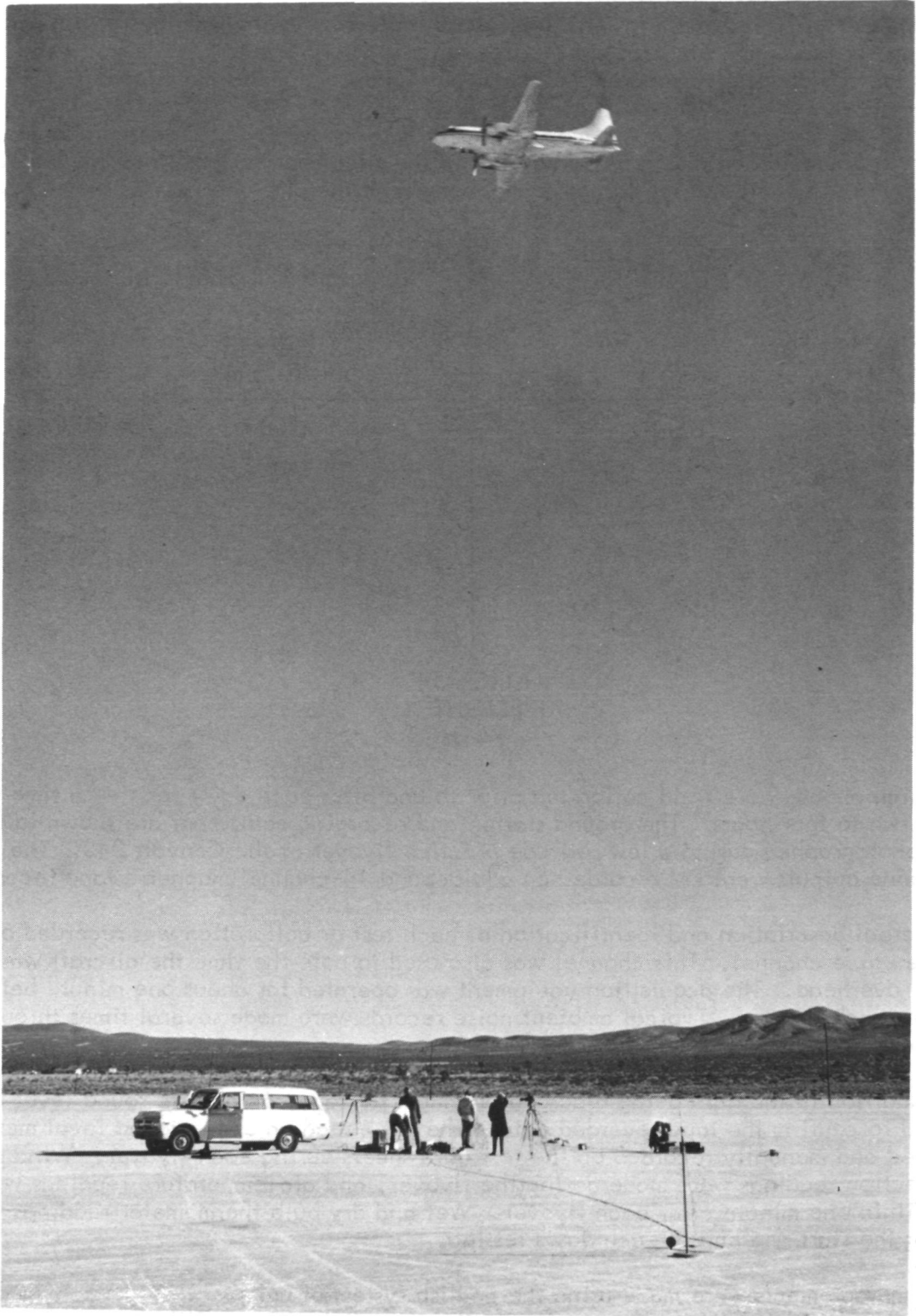ded by a battery-converter combination. The batteries were kept fully charged by a portable generator unit operated between data runs.

Figure 8 is a schematic diagram of the data acquisition instrumentation. The Bruel and Kjaer (B & K) electronic voltmeters were modified to provide an additional output 20 dB below the regular output. During the on-site microphone calibrations the voltmeters were operated at two different gain settings, one 20 dB higher than the other, in order to permit calibration of both outputs at as high a signal-to-noise ratio as possible. During data acquisition runs the voltmeter gain was set at a value such that the maximum "low" output was just below the maximum allowable input of the tape recording system -- the "high" channel would overload on the maximum signal level. This was done in order to achieve the maximum possible signal-to-noise ratio. During the glider measurements the voltmeters were set for the maximum gain, but the low source signal level precluded overloading the tape system, even on the "high" output channels.

Figure 9 presents a schematic diagram of the data reduction instrumentation. The low gain channel of each microphone system was analyzed for all tests except for the glider flyovers, as previously stated, which required use of the high gain channel.

All of the data were analyzed with the Hewlett-Packard Model 8054A real-time third-octave band analyzer. This instrument has 24 one-third octave band filters covering a range of center frequencies of 50 to 10 000 Hz. Additionally, the Bruel and Kjaer Type 2305 Level Recorder was used to both verify the magnitude of the peak overall sound pressure level and to relate the time at which this occurred to the aircraft overhead position.

The Federal Scientific "Ubiquitous" real-time spectrum analyzer was used to check several spectra for discrete frequencies.

Data Reduction Methods

All of the data were analyzed in terms of one-third octave band sound pressure levels (dB re 2×10^{-5} N/m^2). A "composite" one-third octave band spectrum was obtained from the output signal of each microphone. The analyzer used to obtain these composite levels incorporated a "holding" circuit which would retain (and later print out) the maximum rms value of each one-third octave band that was recorded during the flyover. These data are presented in tabular form in Appendix A. Visual observation of the analyzer's cathode ray tube display, during reduction of the two-engine aircraft data, showed that the low frequencies reached their maximum values before the mid and high frequencies, which peaked simultaneously with the OASPL at the aircraft overhead position. In addition, aural monitoring of the data channels, using high amplifier gain, revealed a definite "rumble" preceding the aircraft for several seconds prior to the overhead position. It is noteworthy that this "rumble" was below the level of audibility at the test site.

B & K NO. 4134 12.7 MM (1/2 IN.)
CONDENSER MICROPHONES WITH
B & K NO. VA0082 WINDSCREENS

B & K NO. 2619 FET
PREAMPLIFIERS

HIGH
OUTPUT

HIGH
OUTPUT

B & K NO. 2409 ELECTRONIC
VOLTMETERS

LOW
OUTPUT
(-20 dB)

LOW
OUTPUT
(-20 dB)

VOICE
CHANNEL

AMPEX FR-1300
14 CHANNEL
MAGNETIC TAPE
RECORDER
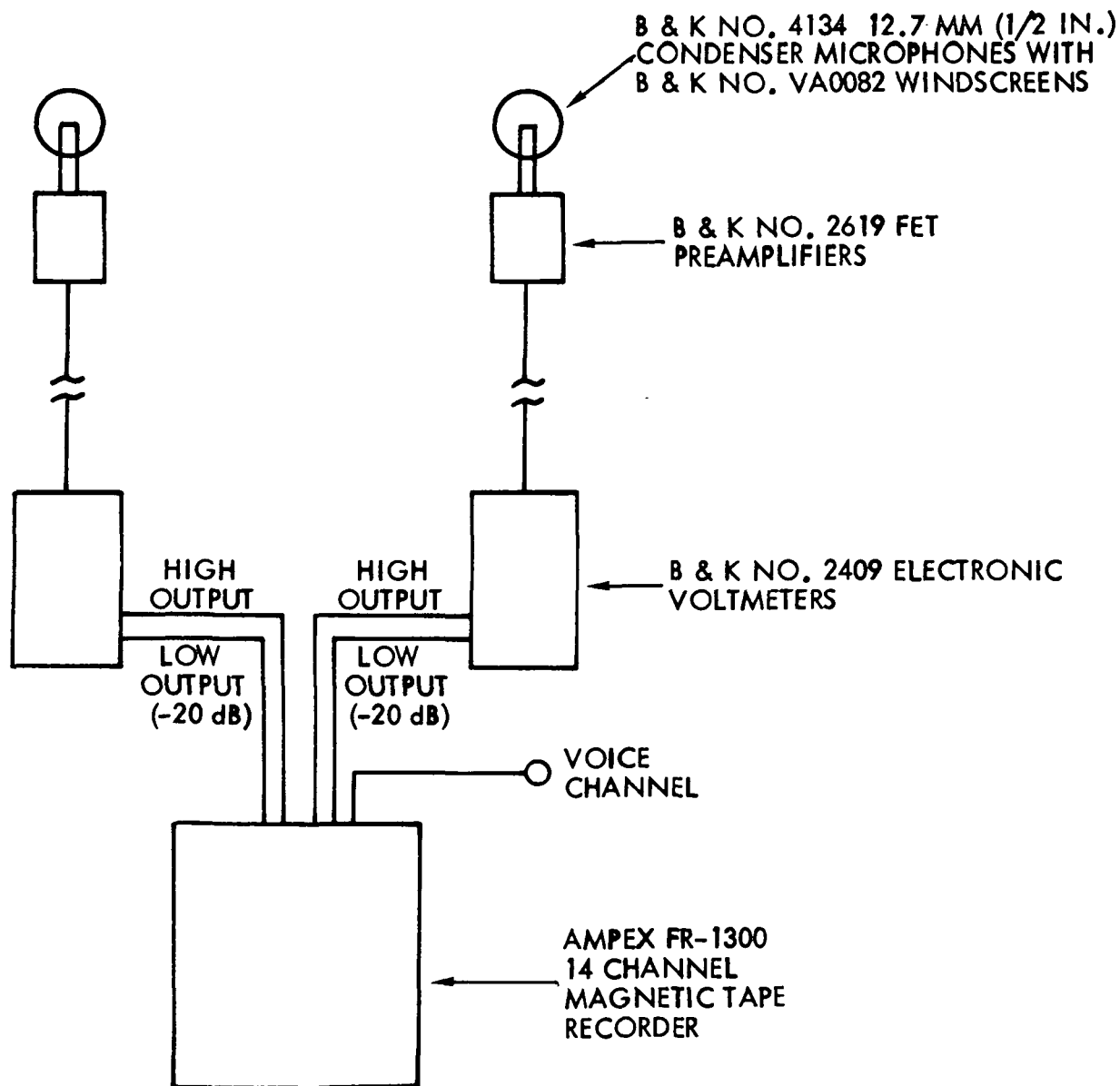
Figure 8. - Data Acquisition Instrumentation

SANBORN
MODEL 3924A
TAPE SYSTEM

H-P NO. 8054A
REAL-TIME
AUDIO SPECTRUM
ANALYZER WITH
PRINTER

B & K NO. 2305
LEVEL RECORDER
(TIME-HISTORIES)

FEDERAL SCIENTIFIC
UA-7AU/D "UBIQUITOUS"
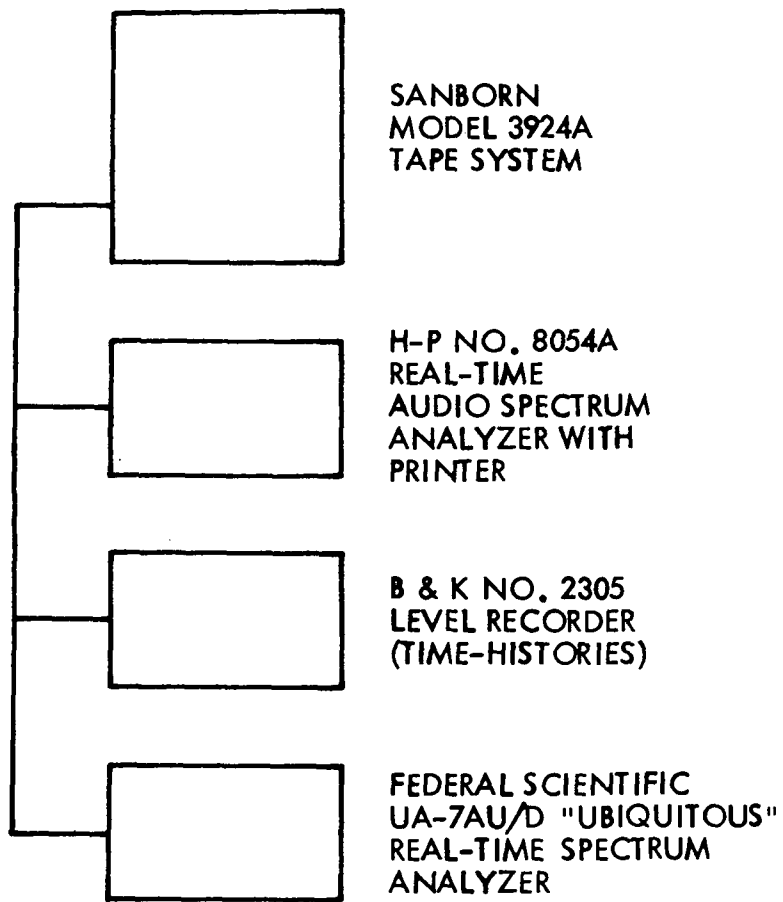REAL-TIME SPECTRUM
ANALYZER

Figure 9. – Data Reduction Instrumentation

15

The one-third octave band analyzer was also operated in a "continuous" printout mode for two selected runs. Each of the 24 one-third octave band levels were printed out every 1.2 seconds. The total operation time was about one minute per run. This "continuous" mode analysis confirmed the maximum SPLs obtained from the composite analyses and are not reported further.

Maximum rms sound pressure levels from the two microphones were averaged to account for off-centerline flight paths. The resulting one-third octave band levels were then normalized to an altitude of 152.4 meters (500 feet) by accounting for spherical spreading and atmospheric absorption. Corrections for atmospheric absorption used the on-site measured values of air temperature and relative humidity and the corresponding absorption coefficients from reference 10.

The normalized one-third octave band levels were then summed on an energy basis to determine the overall sound pressure level (OASPL) from the composite spectra. The maximum rms level from each of the 24 one-third octave bands did not always occur as the aircraft passed directly over the microphones nor did all of the maxima occur at the same time. In general, the low frequency bands reached their peak values prior to the aircraft being directly over the microphones, whereas the mid and high frequency bands reached their maximum values at, or slightly after the overhead position, as mentioned above. These effects are attributable to the directivity of the various sources contributing to the total aerodynamic noise spectrum, the influence of atmospheric absorption on the mid and high frequencies, and the Doppler effect. The OASPL was also determined directly by measuring the maximum rms value for each microphone with the level recorder and averaging the results. The OASPL time histories from the level recorder showed that the OASPL reaches its peak level at approximately the overhead position. In a third method, the maximum OASPL during each flyover was read directly from the on-site sound level meter. The three OASPLs determined from the three methods are presented in Table II and discussed in the Test Results section.

In general, the OASPLs from the three methods were in good agreement for all but a few of the runs. The composite OASPLs from the summation of the one-third octave band levels appeared to give the most consistent results and were used in the analyses.

Although the glider flyovers were made at altitudes lower than those for the other aircraft, the resulting SPLs were nevertheless close to, or lower than the SPLs of the ambient noise -- particularly for the low speed flyovers and at low frequencies. Since the low frequency bands of the glider data had the highest SPLs, they determined the OASPL value; consequently special procedures were used in reducing the glider data. The one-third octave band levels of the ambient noise, before and after each test, were analyzed and averaged. Whenever the average ambient noise levels were at or below those of the total noise measured, the effects of the ambient noise were removed from the total noise by the method of energy subtraction. In those few cases where the ambient levels were above the measured noise levels the values were set at "0" (see Appendix A). The resulting "signal-only" SPLs were then normalized to an altitude of 152.4 meters (500 feet) using spherical spreading and atmospheric absorption corrections as previously described. The composite OASPL was then obtained by energy summation of the normalized "signal-only" one-third octave band levels. It was not necessary to apply these procedures to the data from the other aircraft since the signal-to-ambient noise ratio was

16

TABLE II

MEASURED MAXIMUM OVERALL SOUND PRESSURE LEVELS AT 152.4 METERS ALTITUDE

Aircraft	Test Run No. (n)	Velocity		Overall Sound Pressure Level, dB		
		m/sec	knots	Composite	Time History	On-site Meter Reading
Convair 240	1*	98.52	191.5	82.9	83.8	84
	2*	90.18	175.3	82.7	82.6	83
	3*	82.0	159.4	80.5	80.8	81
	4*	75.11	146.0	79.2	79.6	80
	5**	97.08	188.7	82.7	83.3	81
	6**	85.71	166.6	82.2	82.6	81
	7**	77.84	151.3	79.3	81.7	78
Douglas DC-3	8*	76.29	148.3	78.5	78.3	77
	9*	65.18	126.7	74.8	75.6	76
	10*	55.41	107.7	71.4	71.3	70
	11**	75.88	147.5	79.6	78.8	79
	12**	66.88	130.0	76.1	72.8	76
	13**	55.77	108.4	72.3	71.7	76
Aero-Commander Shrike	14*	89.72	174.4	75.4	76.2	83
	15*	78.71	153.0	72.3	73.6	78
	16*	69.45	135.0	71.4	74.1	88
	17*	58.60	113.9	70.2	70.4	--
	18**	81.59	158.6	73.1	73.7	76
	19**	70.58	137.2	72.7	74.0	73
	20**	62.40	121.3	68.9	69.9	71
Prue-2	21*	51.34	99.8	57.5	64.0	61
	22*	42.08	81.8	48.4	--	--
	23*	32.77	63.7	48.2	--	57
	24**	51.39	99.9	59.5	59.7	60
	25**	42.13	81.9	50.5	--	58
	26**	30.40	59.1	55.9	--	55
Cessna 150	27*	46.66	90.7	66.5	66.3	--
	28*	29.89	58.1	53.8	--	--

* Light gross weight } see Table I
** Heavy gross weight)

in excess of 10 dB for all frequency bands except at the extreme low and high ends of the frequency spectrum. The 10 dB value is used because the energy summation of two noise levels differing by 10 dB results in a total level only 0.4 dB higher than the highest of the two separate sources. Adjustments for the ambient noise were not applied to the levels at the extremes of the frequency spectrum since they had no significant influence on the OASPL.

Constant narrow bandwidth analyses were made on at least one run of each aircraft type in order to determine whether discrete tones were present. An analyzer bandwidth of 0.61 Hz was used to cover the frequency range from 5 to 600 Hz and a bandwidth of 9.75 Hz for the frequency range from 200 to 10 000 Hz.

Test Results

The methods and procedures used in reducing the test data were described in detail in the previous section. Briefly, the flyover noise data were reduced in one-third octave bands using a spectrum analyzer whose output gave the maximum rms one-third octave band levels that occurred during the flyover. This is called the "composite" one-third octave band spectrum since the various bands reach their maximum values at different times. An "instantaneous" one-third octave band spectrum would be that spectrum that existed at any one time and would have band levels at or below those of the "composite" spectrum. In addition to the one-third octave band analyses, time histories of the OASPL were made of each test case, and a narrow bandwidth analysis of at least one case for each aircraft was performed to determine whether discrete tones were present in the frequency spectra. A discussion of the results from each of these analyses is presented in the following paragraphs.

Two typical ambient noise spectra are shown in figure 10. The composite one-third octave band spectra for each run are shown in figures 11 through 15. Each figure, except figure 15, presents the light and heavy weight flights on separate graphs for clarity. In general, the one-third octave band spectra increase in level with increasing velocity while increases in gross weight, at the same velocity, do not appear to increase these spectral levels significantly.

In all cases, except the glider, the signal levels were much higher than the ambient noise levels and therefore could be used directly. During the reduction of the glider data, ambient noise level recordings taken before and after each run were also reduced. The maximum, minimum, and average values of these data are shown in figure 14(C). In an attempt to compensate for the high ambient noise levels, the average ambient noise for each run was removed from the flyover noise levels of that run using the method of energy subtraction. In spite of these corrections, the data (figure 14) are still questionable in the low frequencies due to the relatively large fluctuations of the ambient noise in these frequency bands. This is particularly true for the low velocity runs. The uncertainty of the level of the glider noise in these low frequencies which control the OASPL results in a larger OASPL scatter than for the other aircraft in this study.
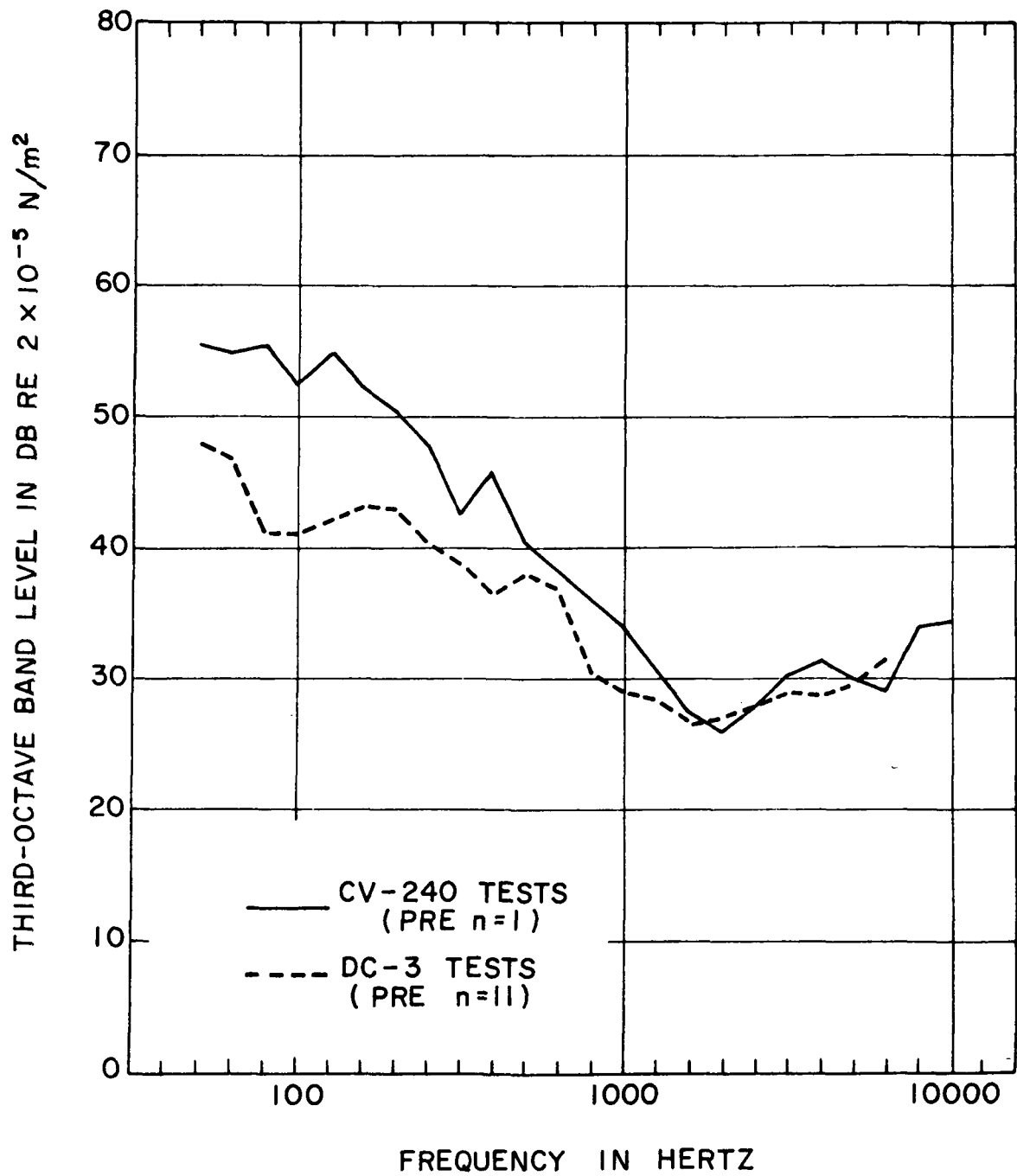
Figure 10. – Typical Ambient Noise Spectra
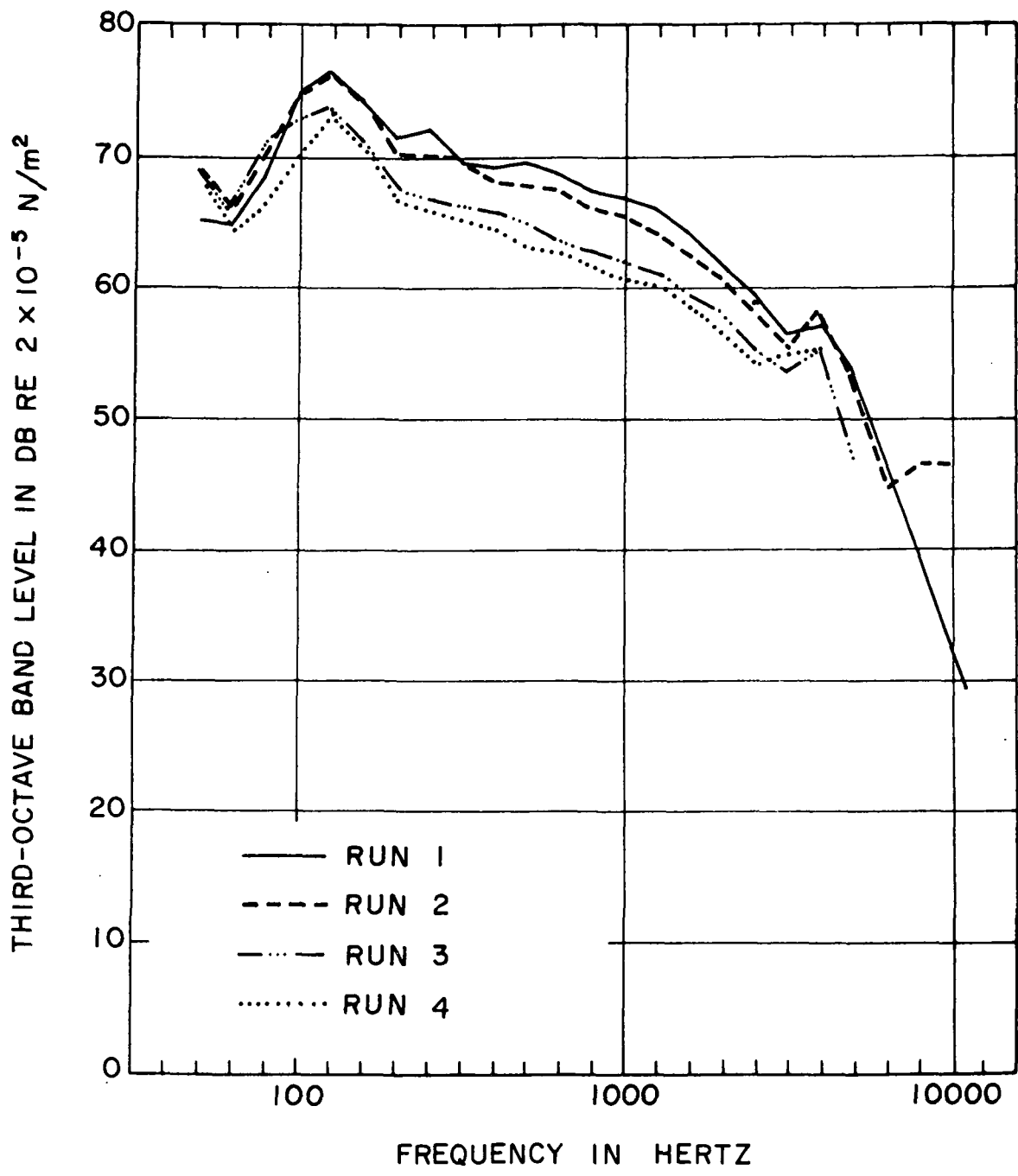
Figure 11(A). – Convair 240 Measured Noise Spectra – Light Gross Weight
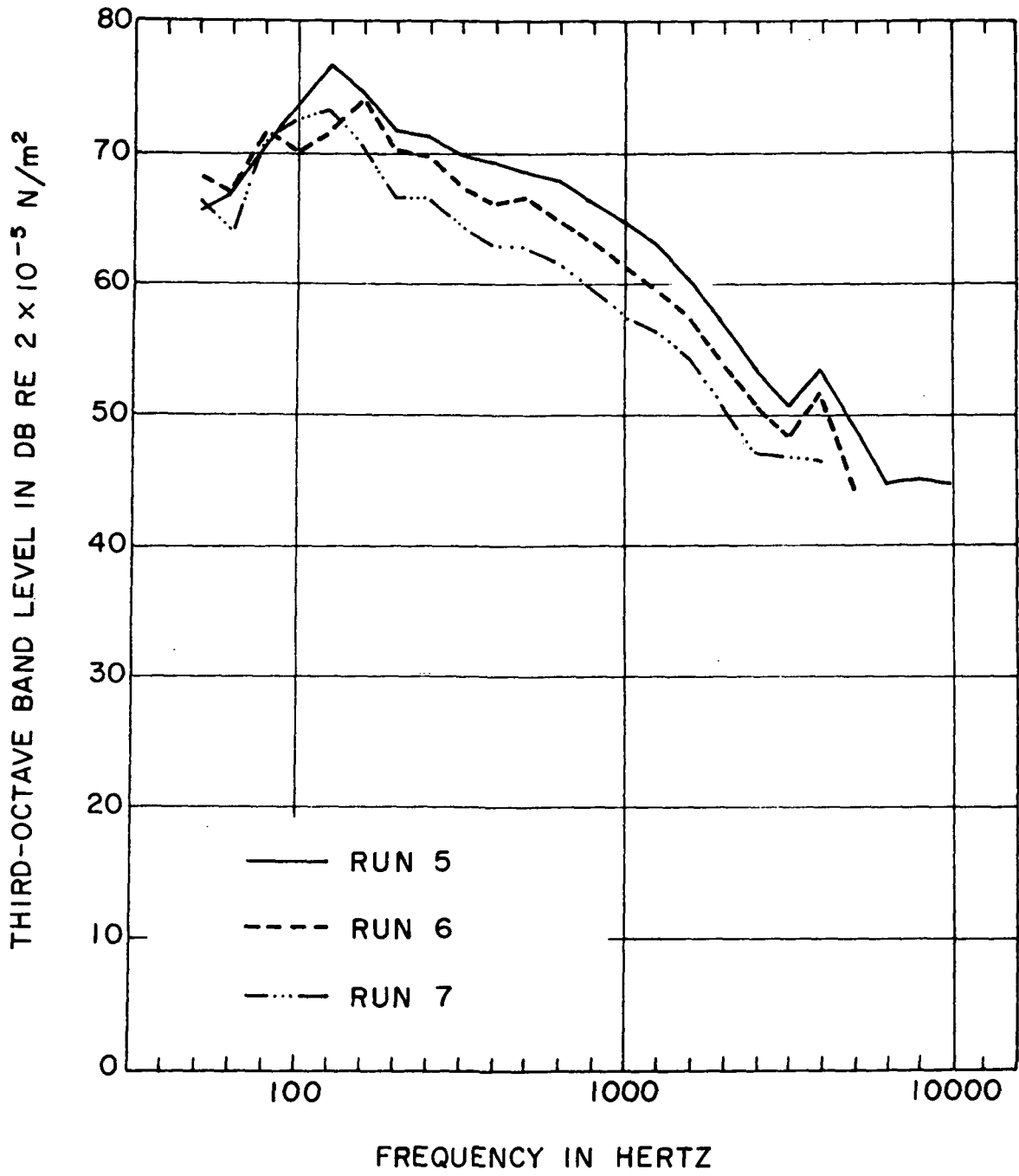
Figure 11(B). Convair 240 Measured Noise Spectra - Heavy Gross Weight
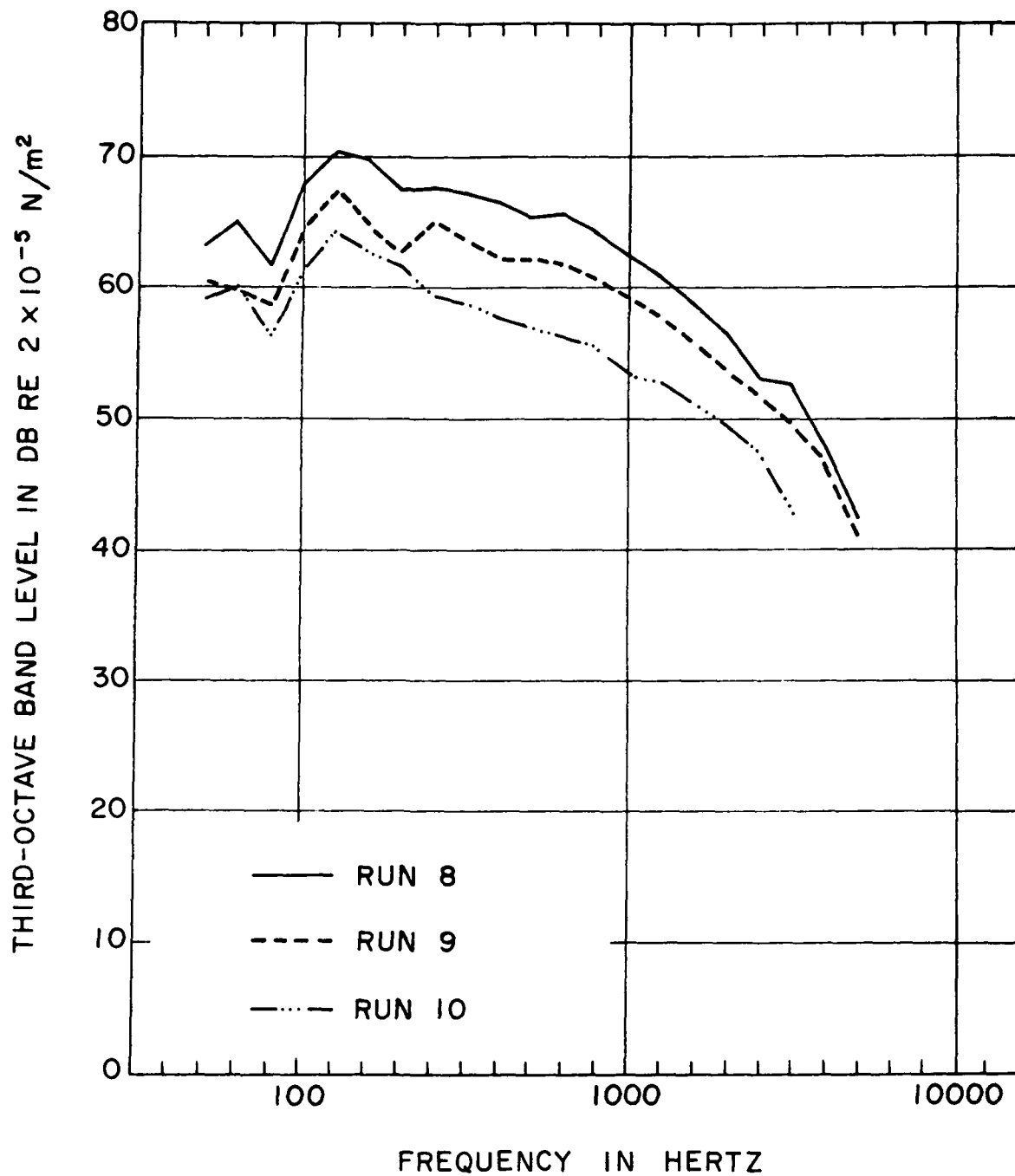
Figure 12(A). – Douglas DC-3 Measured Noise Spectra – Light Gross Weight
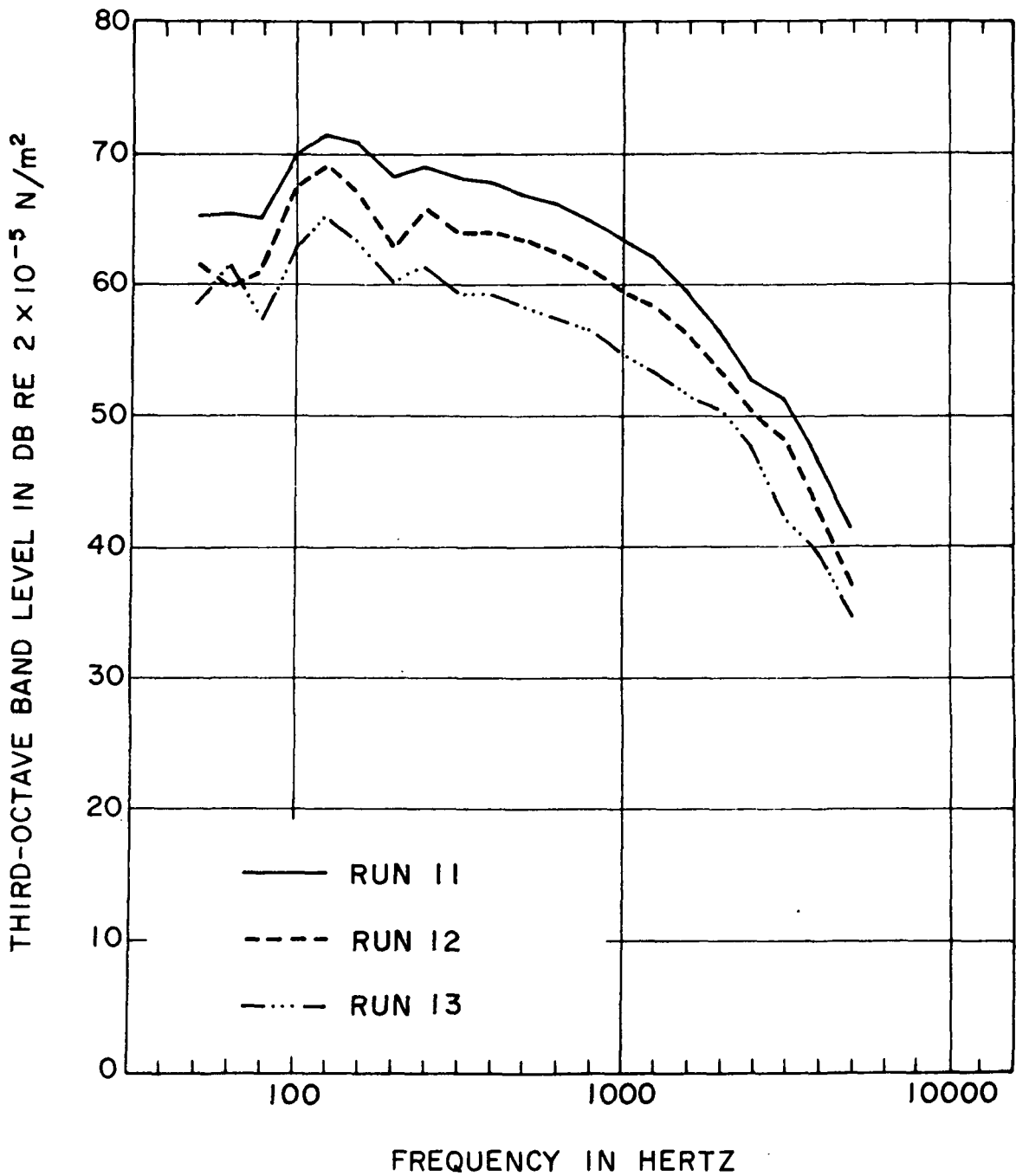
Figure 12(B). – Douglas DC-3 Measured Noise Spectra – Heavy Gross Weight

Figure 13(A). – Aero-Commander Shrike Measured Noise Spectra – Light Gross Weight

Figure 13(B). – Aero–Commander Shrike Measured Noise Spectra – Heavy Gross Weight

25

Figure 14(A). – Prue-2 (Glider) Measured Noise Spectra – Light Gross Weight
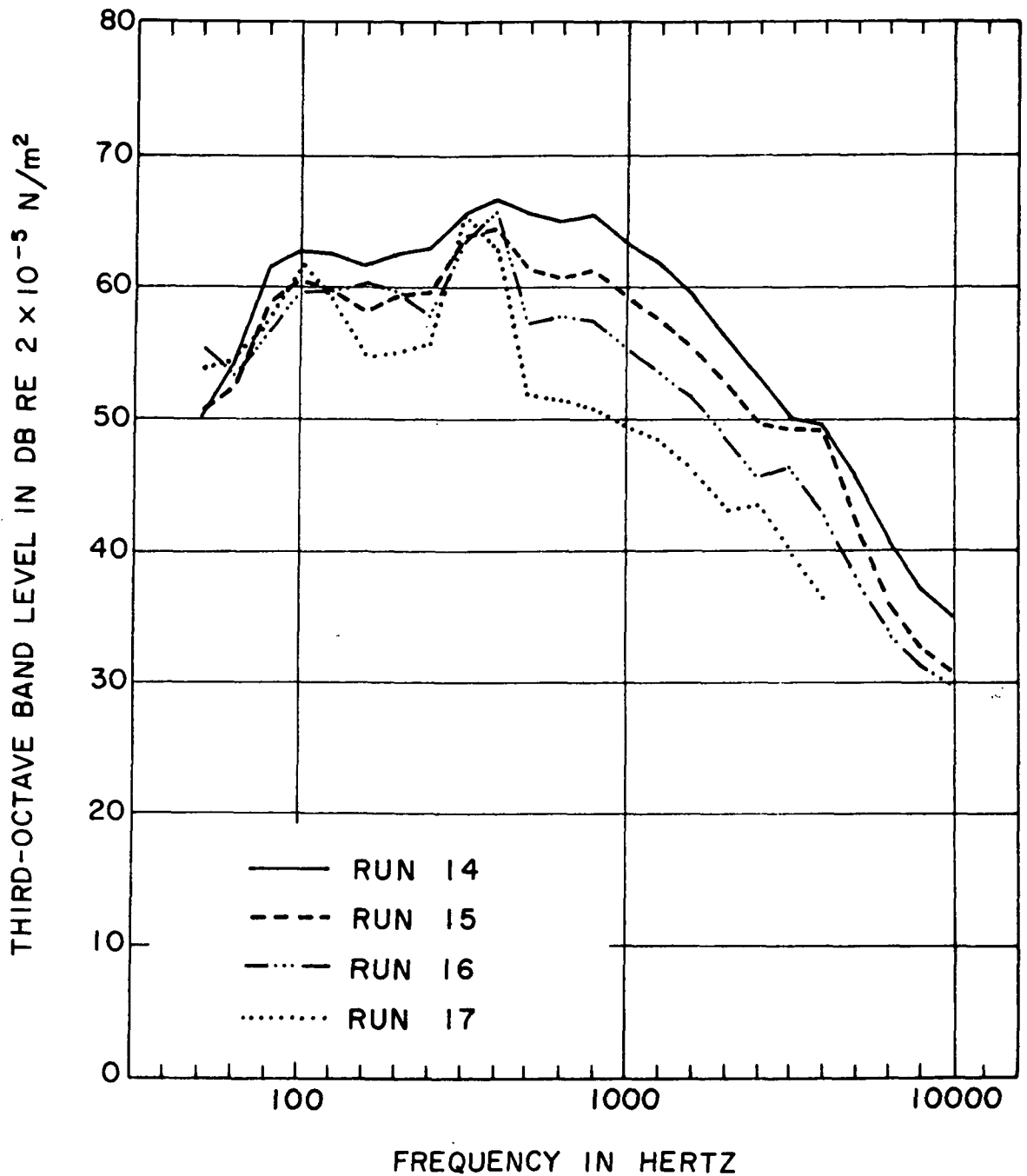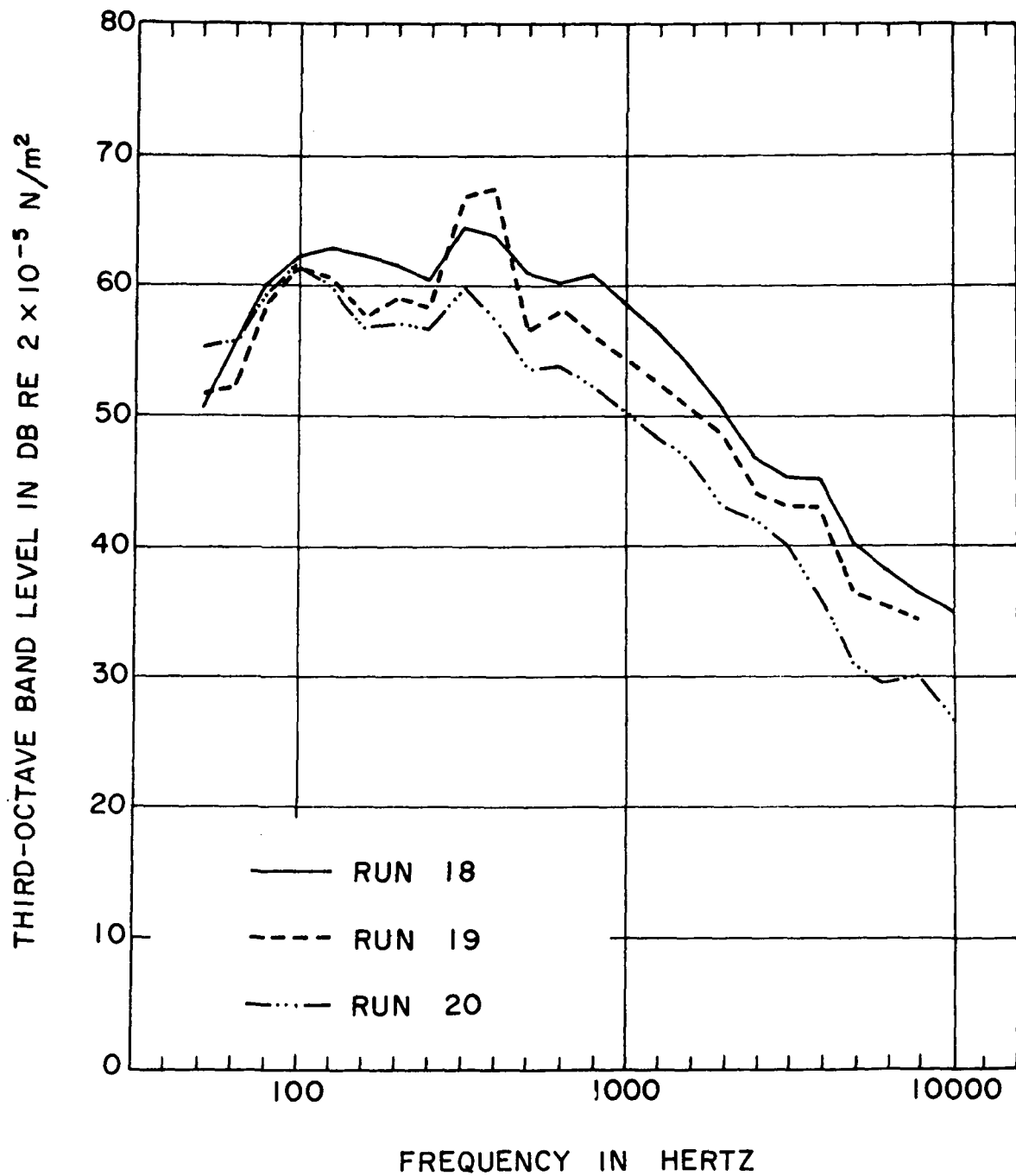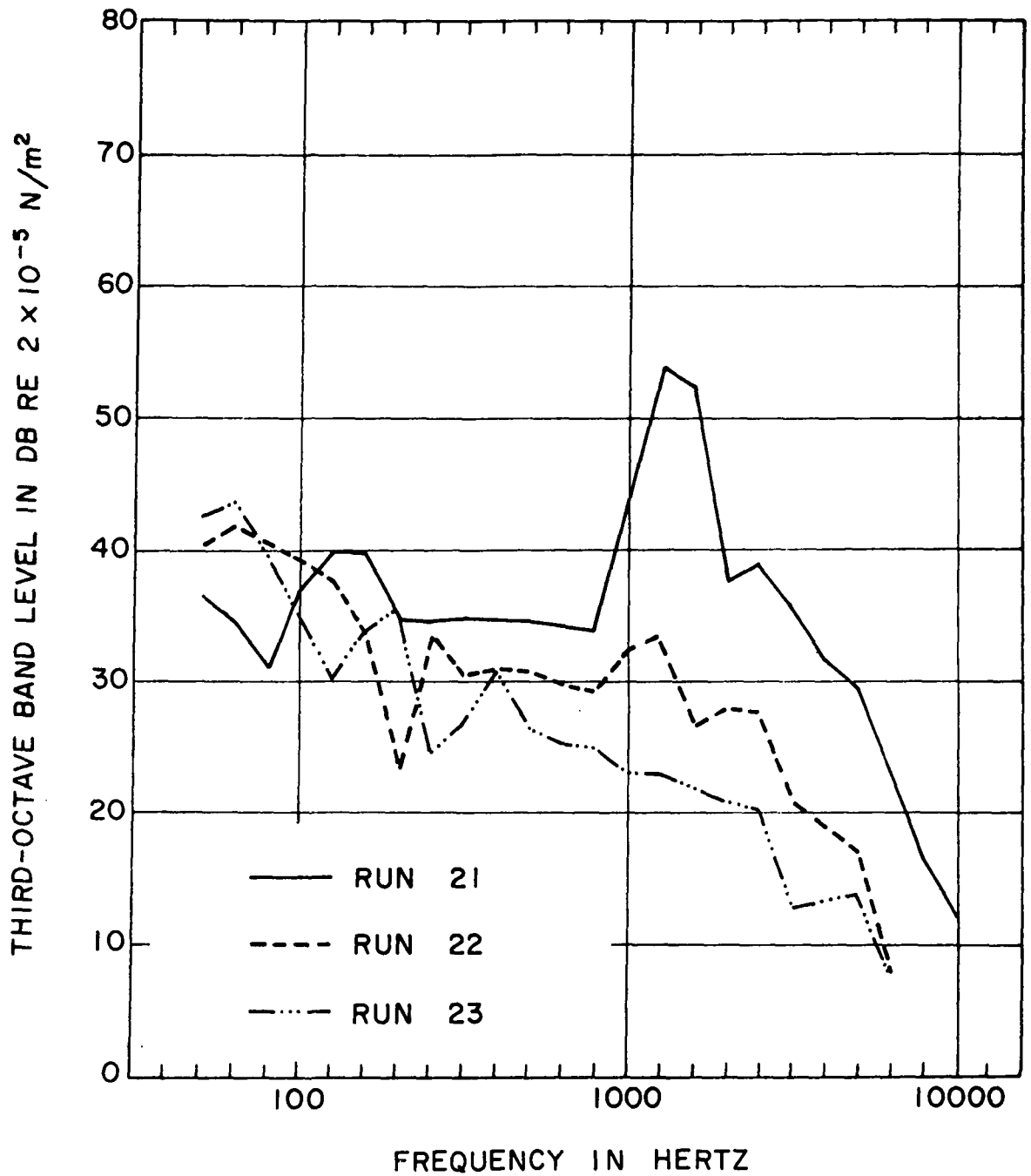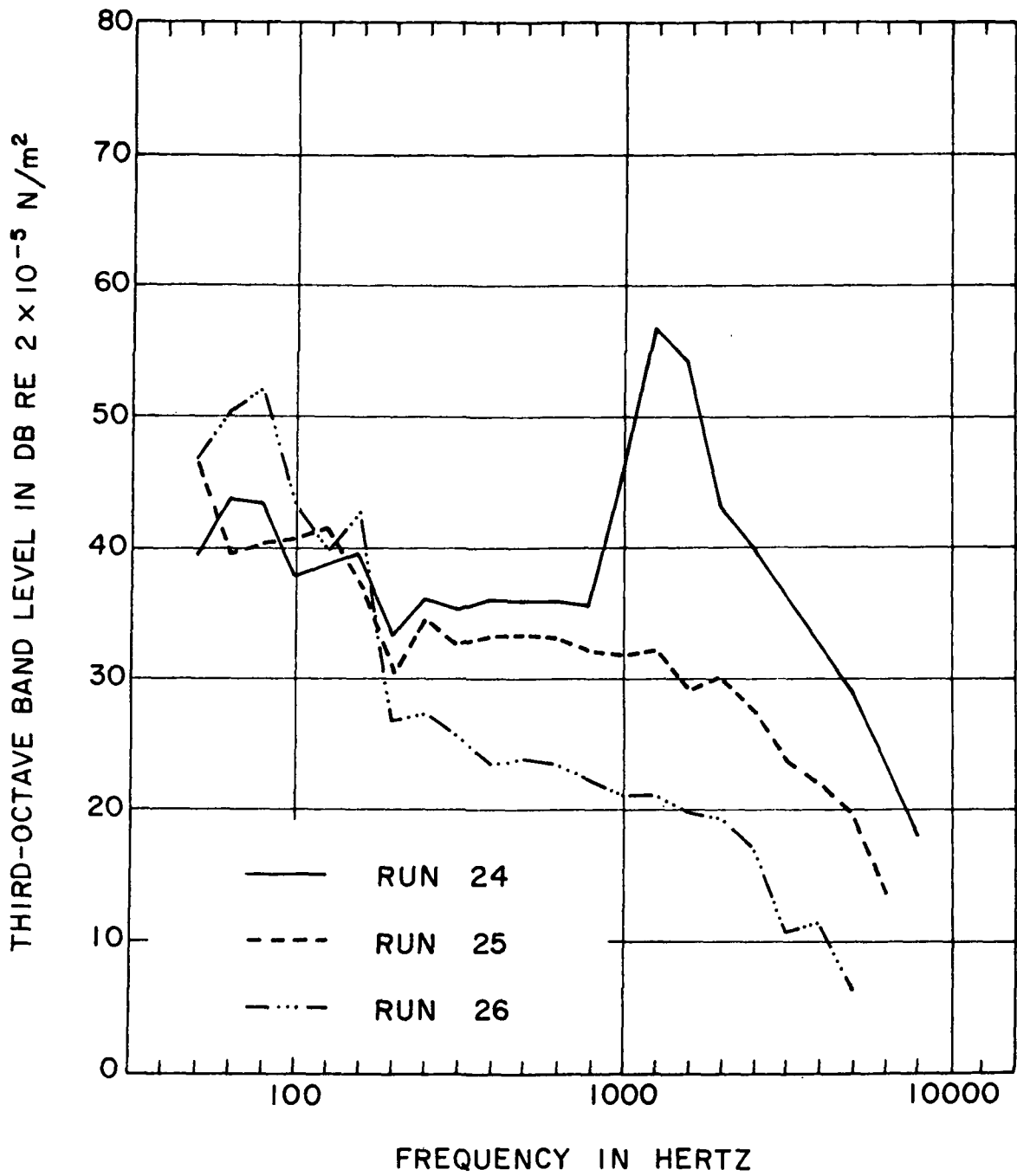
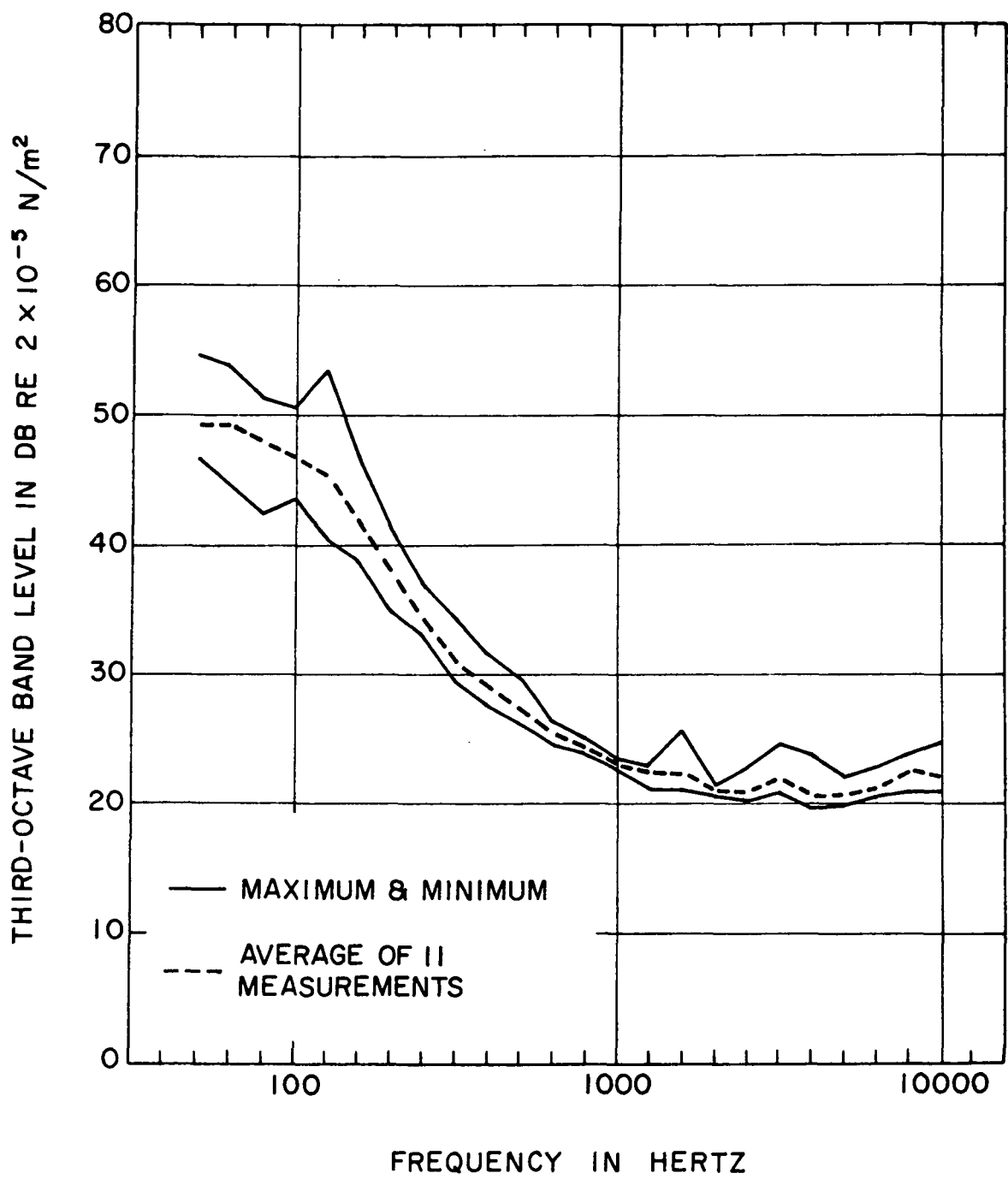Figure 14(B). – Prue-2 (Glider) Measured Noise Spectra – Heavy Gross Weight

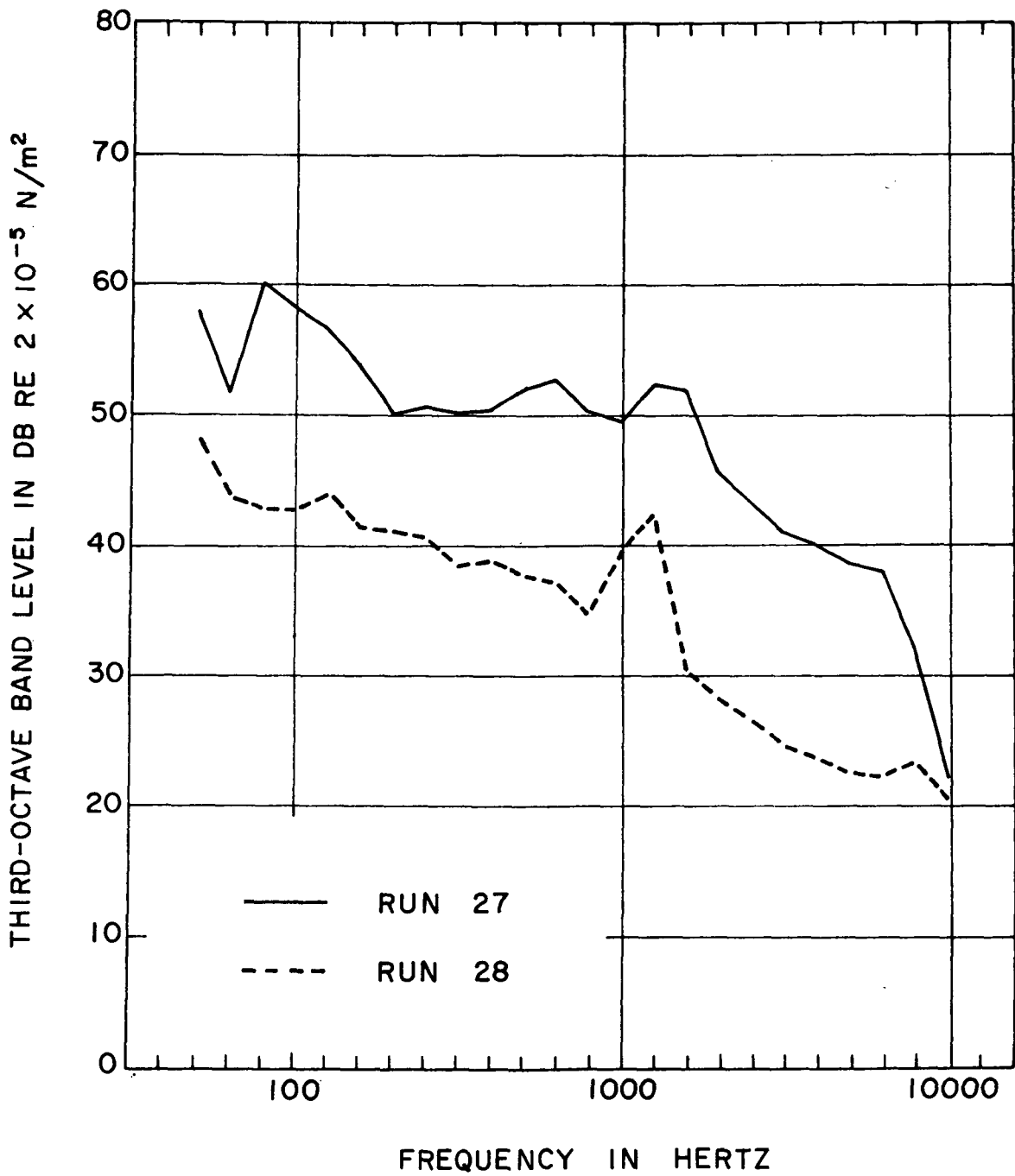Figure 14(C). – Prue-2 (Glider) Ambient Noise Spectra

Figure 15. - Cessna 150 Measured Noise Spectra

The Convair 240 and the Douglas DC-3 (figures 11 and 12, respectively) have the "smoothest" one-third octave band spectra. The spectra for the Aero-Commander Shrike show a number of interesting phenomena. In figure 13(A) a tone is evident between 315 and 400 Hz; the level of this tone decreases with increasing velocity. In figure 13(B), however, the maximum level of this tone occurs at an intermediate velocity. The behavior of this latter case is the same as that of Aeolian tone amplification which results when the vortex shedding frequency of a body coincides with that of the first bending mode of the body. The OASPLs of the high velocity glider runs are dominated by a strong tone which appears in both the 1250 Hz and 1600 Hz bands due to the Doppler shift effect. During the high velocity Cessna run the propeller was windmilling. The turning of the propeller was clearly heard at the measurement station. This could account for the peaks in the low frequencies; however, the source of the high frequency tone is not known. Determination of the actual source of these "peaks" in the one-third octave band spectra is beyond the scope of the program.

Because the one-third octave band spectra contained a large number of bands whose level was higher than the two adjacent bands, indicating the possible presence of tones or very narrow bands of random noise, the previously mentioned narrow bandwidth analyses were performed on selected runs for all of the aircraft. These analyses showed the peaks in the low frequency one-third octave band spectra of the twin engine aircraft to be a peaking of the broadband acoustic energy. The high frequency peaks were tones or very narrow bands of random noise. The high velocity Prue-2 glider runs were shown to have a nearly pure tone at approximately 1400 Hz. The Cessna high velocity run showed a narrow band of noise at approximately 45 Hz and a broadband "group" of energy covering the 80 Hz to 160 Hz region. Fairly pure tones were evident at 1200 Hz and 1300 Hz for the low and high velocity runs, respectively. These narrow bandwidth analyses were primarily for diagnostic purposes and are not used in the subsequent analytical work.

The OASPL values used in the analysis were those calculated from the composite one-third octave band spectra. As mentioned earlier, time histories of the instantaneous OASPL were made of each data run. The maximum OASPL was read from the time history as a check on that obtained from the one-third octave band analysis. In addition to the aforementioned OASPLs obtained during the data reduction phase, a sound level meter at the test site was read and the level manually recorded as the aircraft passed overhead. The microphone on the sound level meter was not equipped with a windscreen, and as a result the meter responded to small wind gusts; therefore, these OASPL values are considered to be less accurate than those obtained from the other two methods. The OASPLs obtained by these three methods, corrected to an altitude of 152.4 meters (500 feet), are presented in Table II. The composite OASPLs were used in the ensuing analysis for several reasons:

- The frequency range was limited to 50 to 10 000 Hz which removed much of the variability caused by inaudible low frequency energy, such as from small wind gusts, recorded by the wide bandwidth instrumentation.

- The integration, or energy averaging, time was longer for the one-third octave band analyzer than for the time-history analyzer, resulting in a better statistical average of the data.

30

- The time span over which the different one-third octave bands peaked is small, resulting in only small differences between the composite and instantaneous OASPL values.

- The composite OASPL values showed greater consistency than the results from either of the other OASPL analyses.

The composite OASPLs shown in Table II are plotted against the primary variable velocity in figure 16. A line representing a slope of the sixth power of velocity is also presented in this figure. It is readily apparent that the data fit a sixth power relationship between level and velocity which indicates that the source of the far-field radiated aerodynamically generated noise is dipole in nature (ref. 11).

The analysis of these data is presented in the next section.
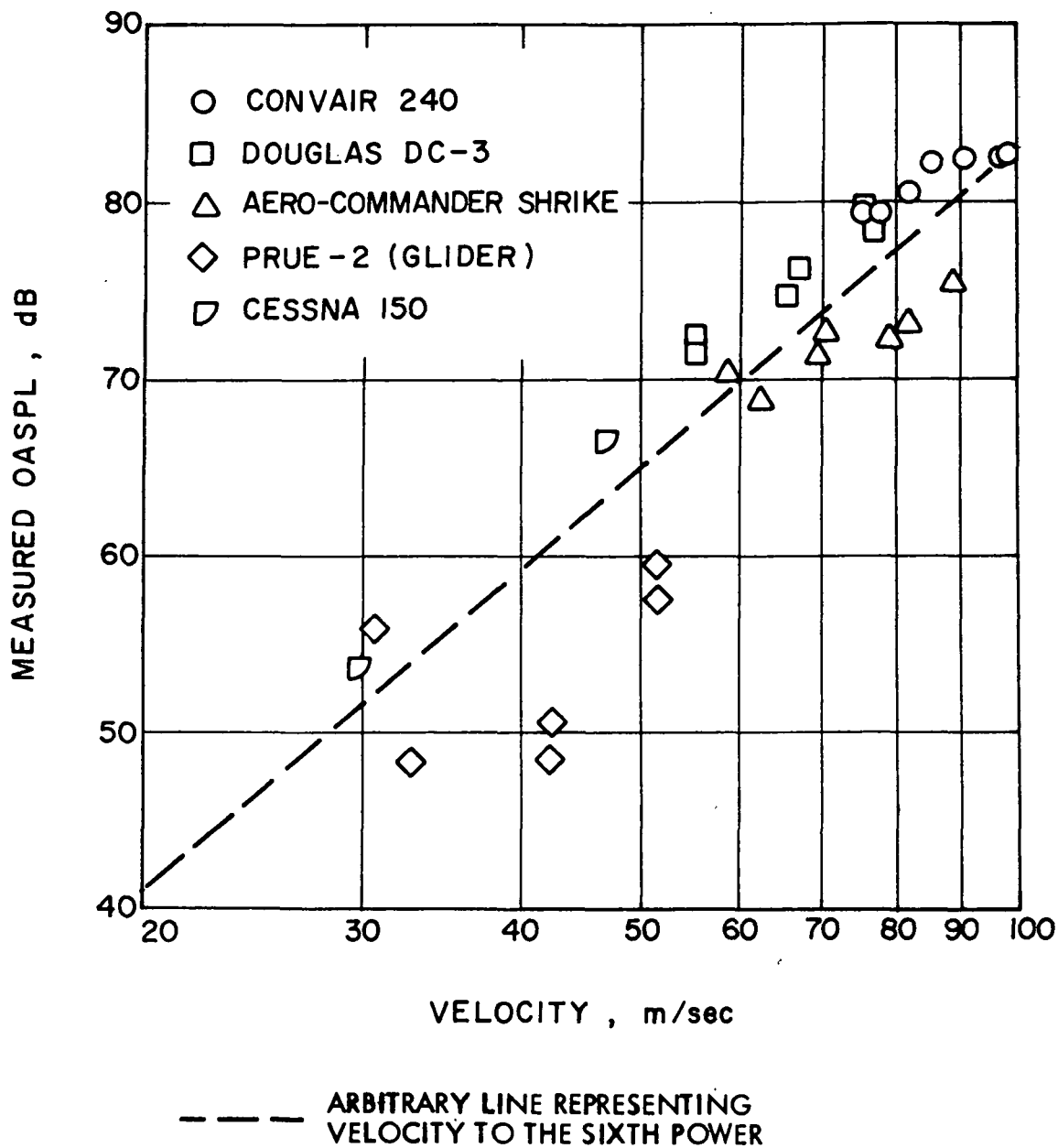
Figure 16. – Effects of Velocity on OASPL

ANALYSIS

General

It was assumed, from the outset, that the source of the far-field radiated aerodynamic noise was essentially the same as that of vortex, or broadband, noise produced by propellers and rotors, viz. dipoles resulting from random fluctuating forces. The primary difference is that the motion involved is rectilinear rather than helical or circular. The dipole nature of the source was established by the sixth power relationship between level and velocity (ref. 11) as shown by the measured data in figure 16. Each elemental area on the surface of the aircraft that experiences a fluctuating force, independent of the actual cause of that disturbance, can be considered a potential source of aerodynamic noise whose radiation pattern is that of a simple dipole. In order to produce a maximum noise level when the aircraft is directly overhead, as was observed during the flight tests, the axis of the dipole must be perpendicular to the flight path. This is the orientation of the dipole associated with the wing lifting force. Dipole radiation resulting from airflow over a surface occurs along the trailing edge. The size of the associated correlation areas is related to the boundary layer thickness which, in turn, is related to the wing chord. The total source area is, therefore, proportional to the wing area. Consequently, it is reasonable to assume that the elemental fluctuating forces associated with the wing lifting force are the major contributors to the far-field radiated, aerodynamically generated noise. The horizontal tail surfaces are also potential contributors to the total vehicle aerodynamic noise spectrum but are considered minor due to their much smaller area in comparison to that of the wings.

Mathematical Model

Having established that the source of the noise is a dipole, it is now necessary to develop a generalized mathematical model to guide the analysis of the data.

The far-field OASPL produced by a moving lift-oriented dipole can be represented by a generalized equation of the form:

$$OASPL = 10 \log_{10}\left[F(\ ) M^6 \left(\frac{\sin\ \phi}{r}\right)^2\right] + \text{constant} \tag{1}$$

where $F(\ )$ is the function relating aircraft parameters to the dipole strength and $\sin \phi$ accounts for the lift dipole radiation pattern. Mach number (M) is used rather than velocity since this accounts for temperature effects, whereas velocity does not. The vehicle parameters contained in $F(\ )$ that can be readily evaluated are W, S, C, b, and combination parameters W/S, W/b, AR. In order to evaluate the influence of these parameters, it is necessary to assume that they act sufficiently independently so that they can be represented by an equation of the form:

$$F(\ ) = W^{X1}\ S^{X2}\ C^{X3}\ b^{X4}\left(\frac{W}{S}\right)^{X5}\left(\frac{W}{b}\right)^{X6}\ (AR)^{X7} \tag{2}$$

33

where the exponents X1 through X7 are evaluated from the measured data. Substituting this expression in equation 1 and separating variables gives:

$$
\begin{aligned}
\text{OASPL} = 10 \Big[&X1 \log W + X2 \log S \\
&+ X3 \log C + X4 \log b \\
&+ X5 \log\left(\frac{W}{S}\right) + X6 \log\left(\frac{W}{b}\right) \\
&+ X7 \log AR + 6 \log M \\
&+ 2 \log\left(\frac{\sin \phi}{r}\right) \Big] + \text{constant}
\end{aligned}
\tag{3}
$$

Use of this equation will be discussed in the Exponent Evaluation section. In order to isolate those effects due solely to the general aerodynamic noise and not peculiar to the individual aircraft, it was necessary to smooth, or idealize, the one-third octave band frequency spectra from which the associated OASPL was obtained by energy summation.

Idealized Spectra

None of the measured aircraft had a uniform, or "smooth," one-third octave band spectrum. Deviations from a smooth spectrum were relatively small for the Douglas DC-3 and Convair 240 but were sizeable for some cases of the Aero-Commander Shrike and Prue-2 glider. The presence of a number of discrete frequencies and relatively narrow bands or "groups" of broadband noise were identified by the previously discussed narrow bandwidth analysis, although determination of the associated noise source(s) was beyond the scope of this study. Potential sources of "discrete" tones, or very narrow bands of random noise, are antennas, pitot tubes, cavities such as wheel wells, the feathered props, separated flow along control surface joints, etc. These "tones" in the frequency spectrum are considered to be characteristic of the individual aircraft and should not be present in an aircraft designed specially for "quiet" operation. Therefore, "smoothed," or idealized, spectra were drawn through the mid and upper frequency bands of the measured spectra; the resulting spectra are presented in figures 17 through 21. New OASPL values were then calculated from these idealized spectra and are presented in Table III. The Prue-2 glider spectra of figure 20 are shown only above about 300 Hz. Below this frequency, interference from ambient noise made the aerodynamic noise spectra uncertain. The calculated OASPLs for the Prue-2 were increased by 3 dB to account approximately for contributions from the undetermined low frequency portion of the spectrum. These calculated OASPL values were used for the evaluation of the exponents of the generalized empirical equation presented in the previous section.
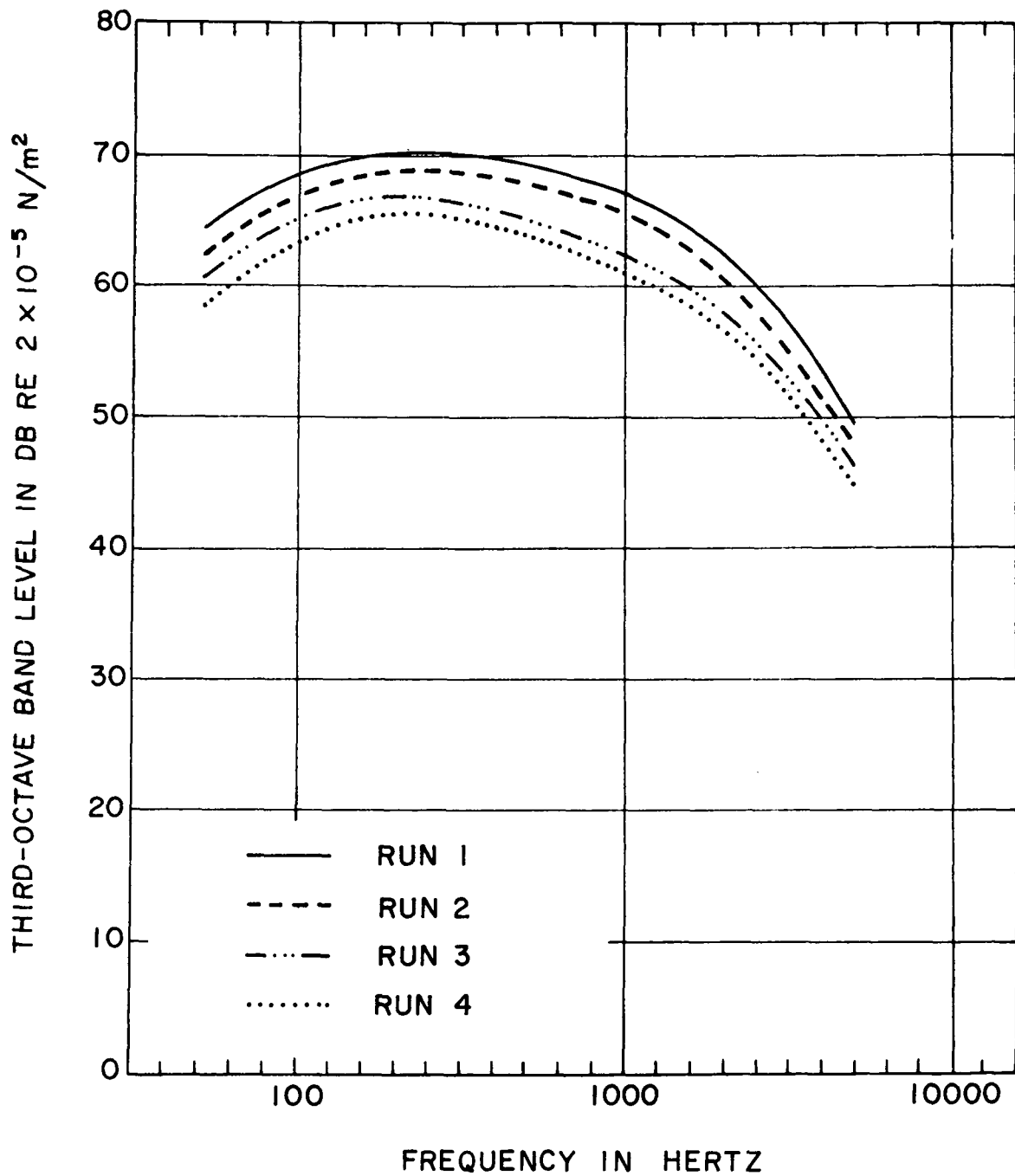
Figure 17(A). – Convair 240 Idealized Noise Spectra – Light Gross Weight
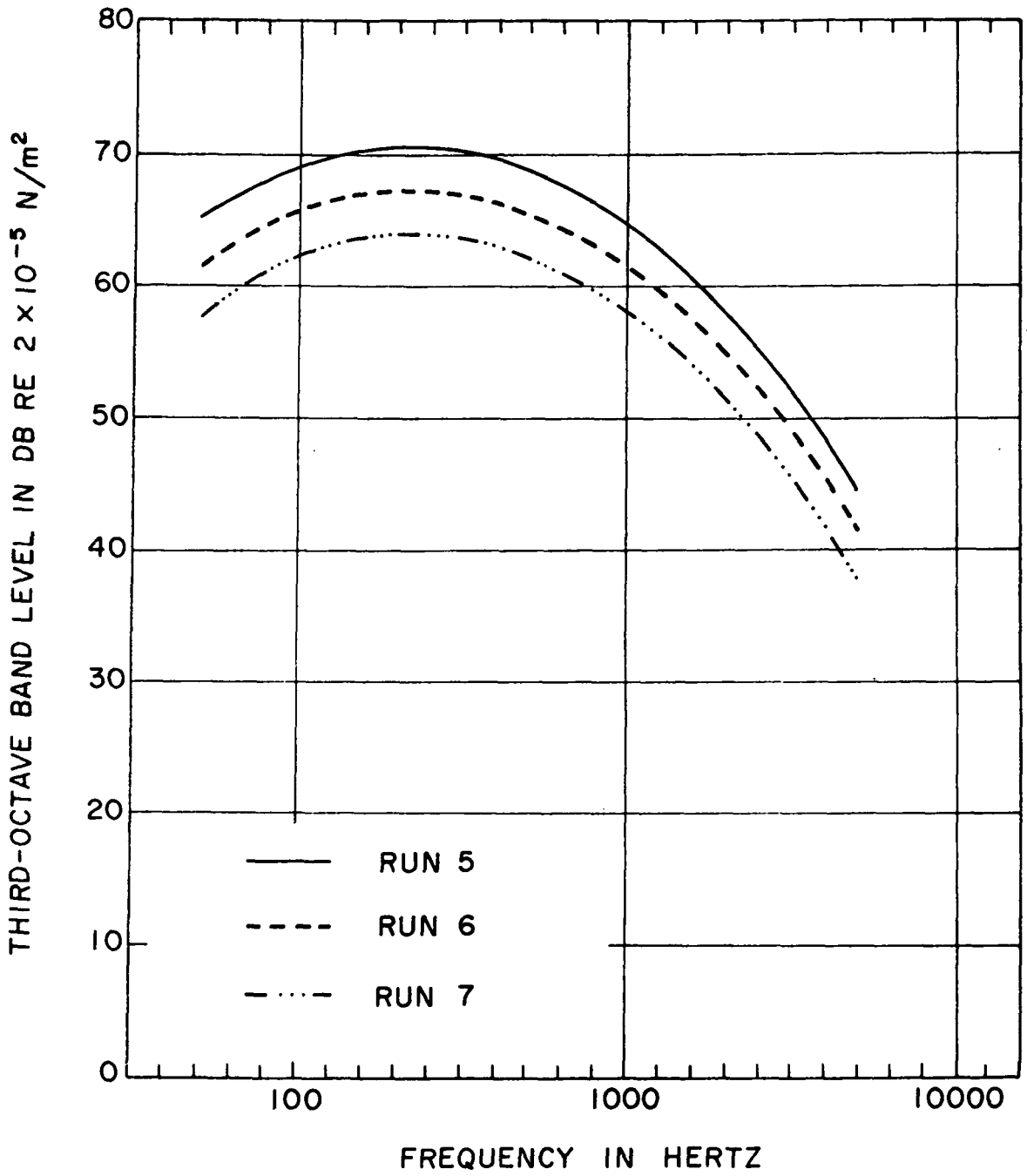
Figure 17(B). – Convair 240 Idealized Noise Spectra – Heavy Gross Weight
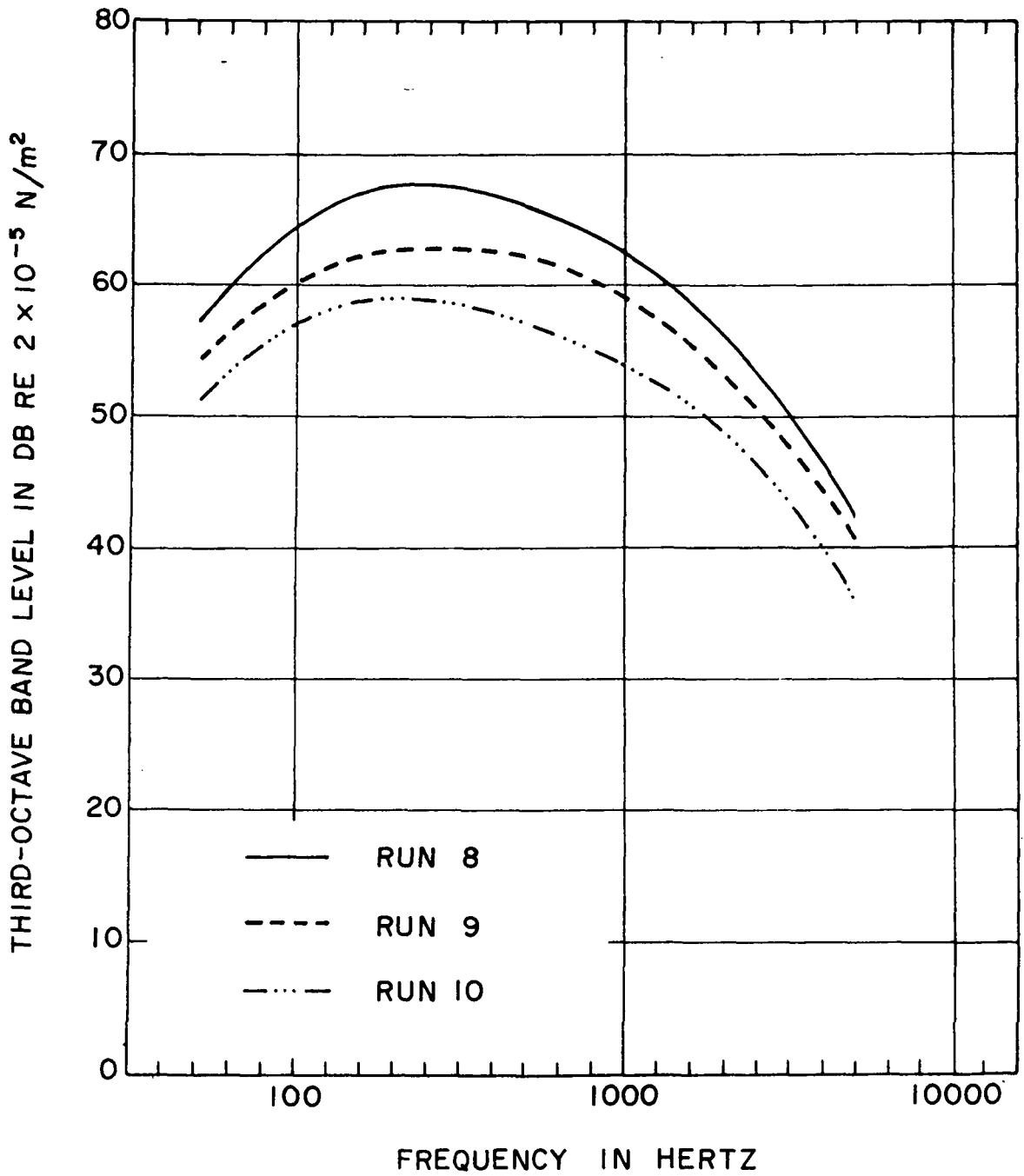
Figure 18(A). – Douglas DC-3 Idealized Noise Spectra – Light Gross Weight
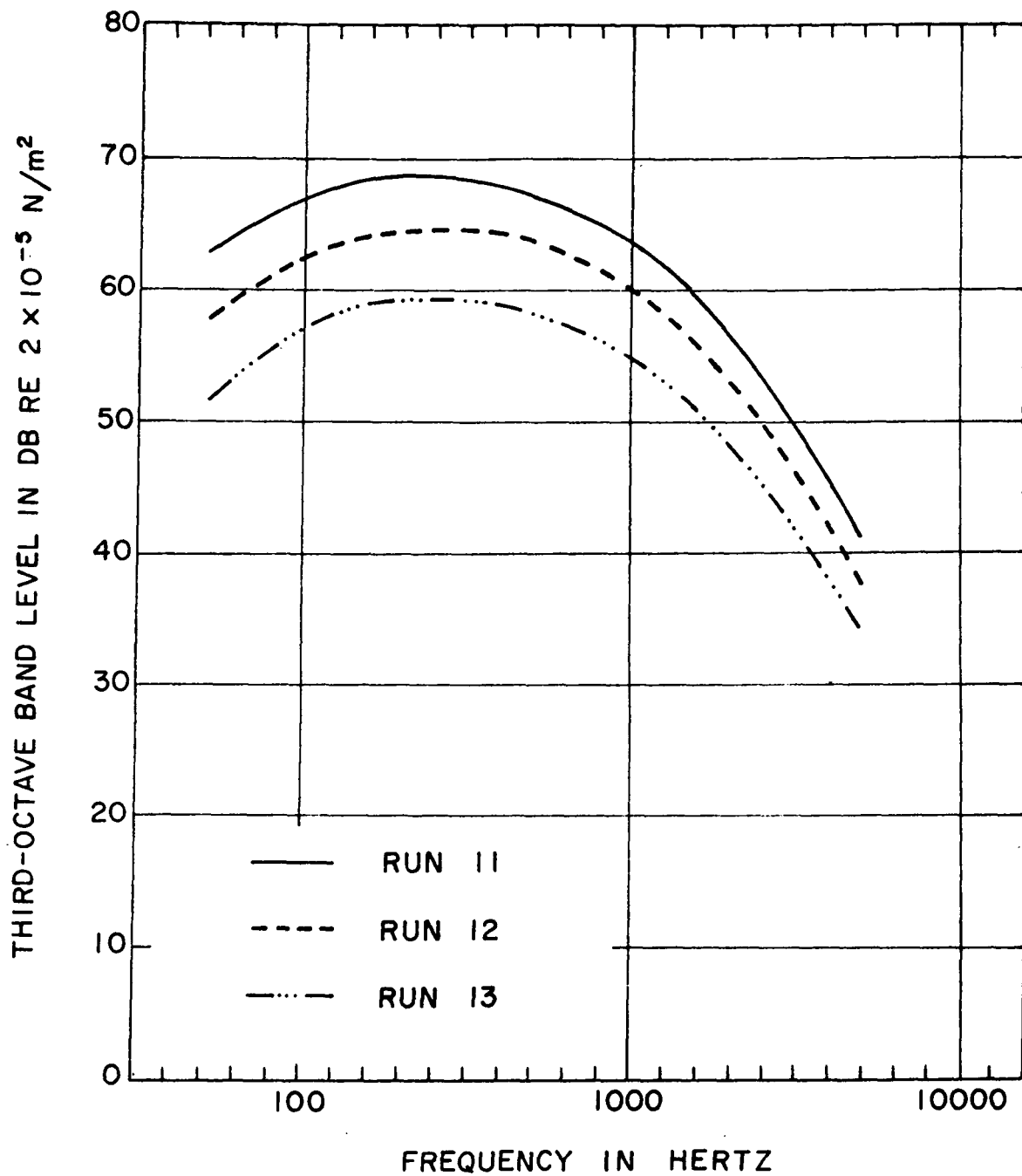
Figure 18(B). – Douglas DC-3 Idealized Noise Spectra – Heavy Gross Weight
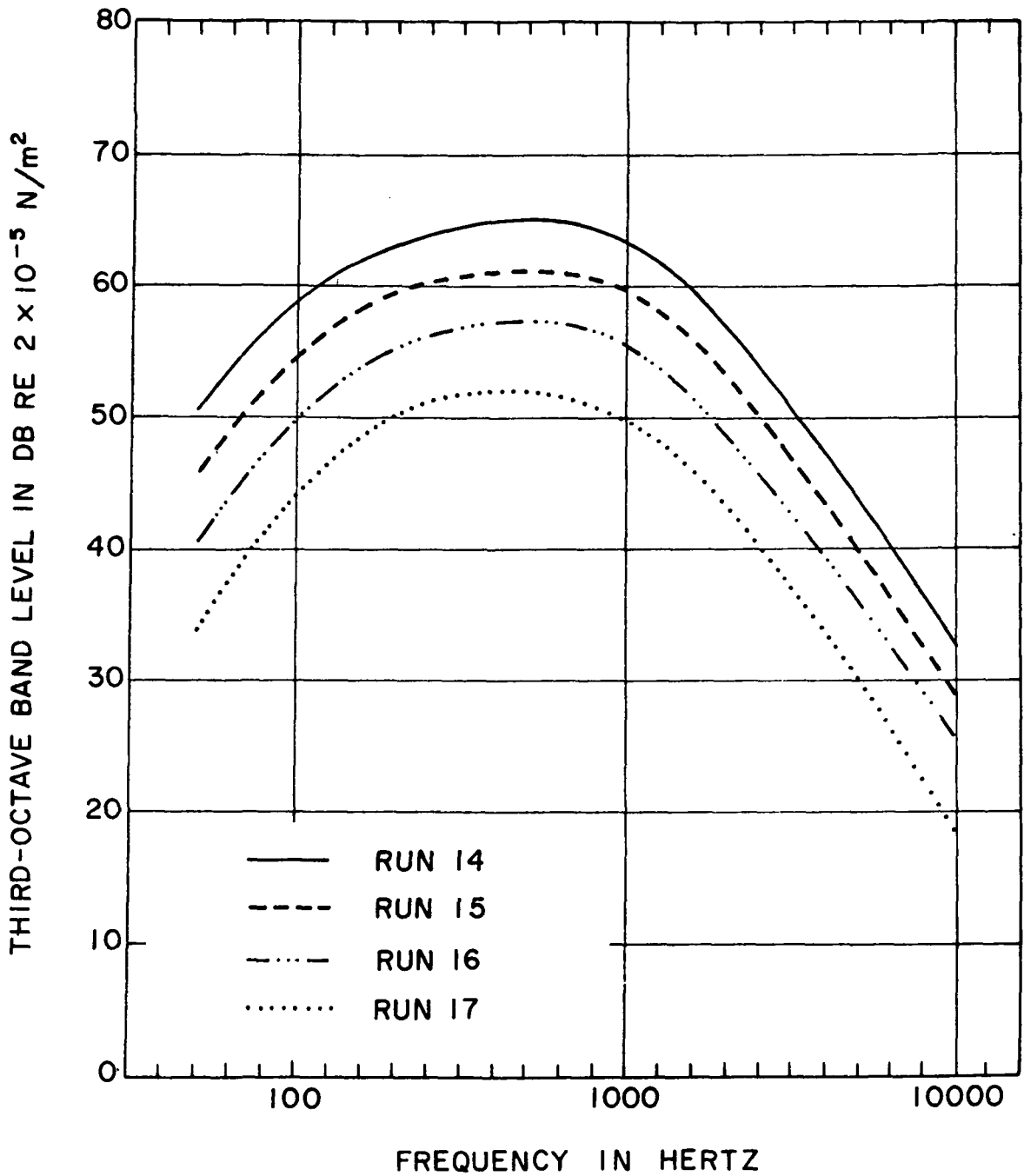
Figure 19(A). – Aero–Commander Shrike Idealized Noise Spectra – Light Gross Weight
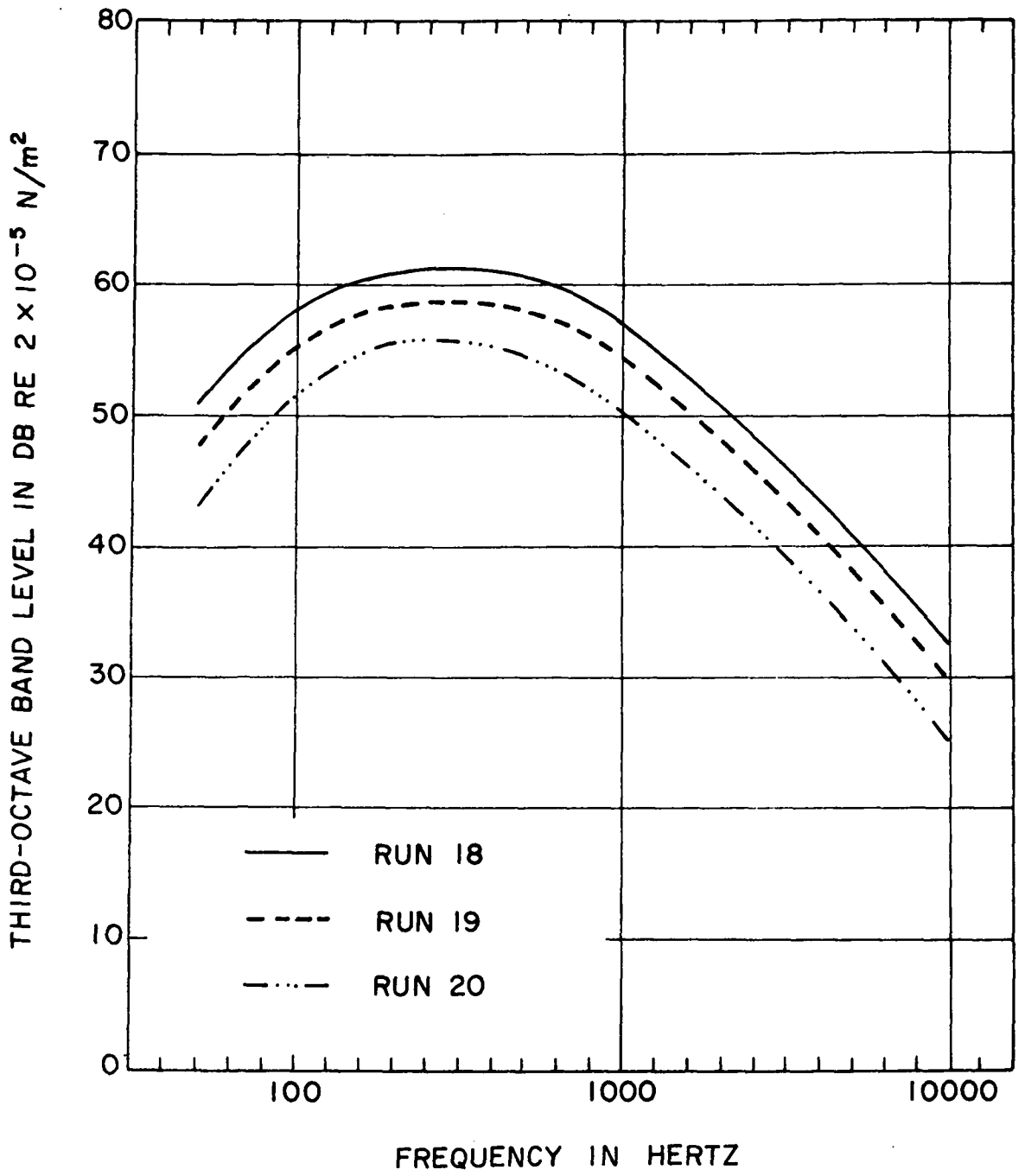
Figure 19(B). – Aero-Commander Shrike Idealized Noise Spectra – Heavy Gross Weight
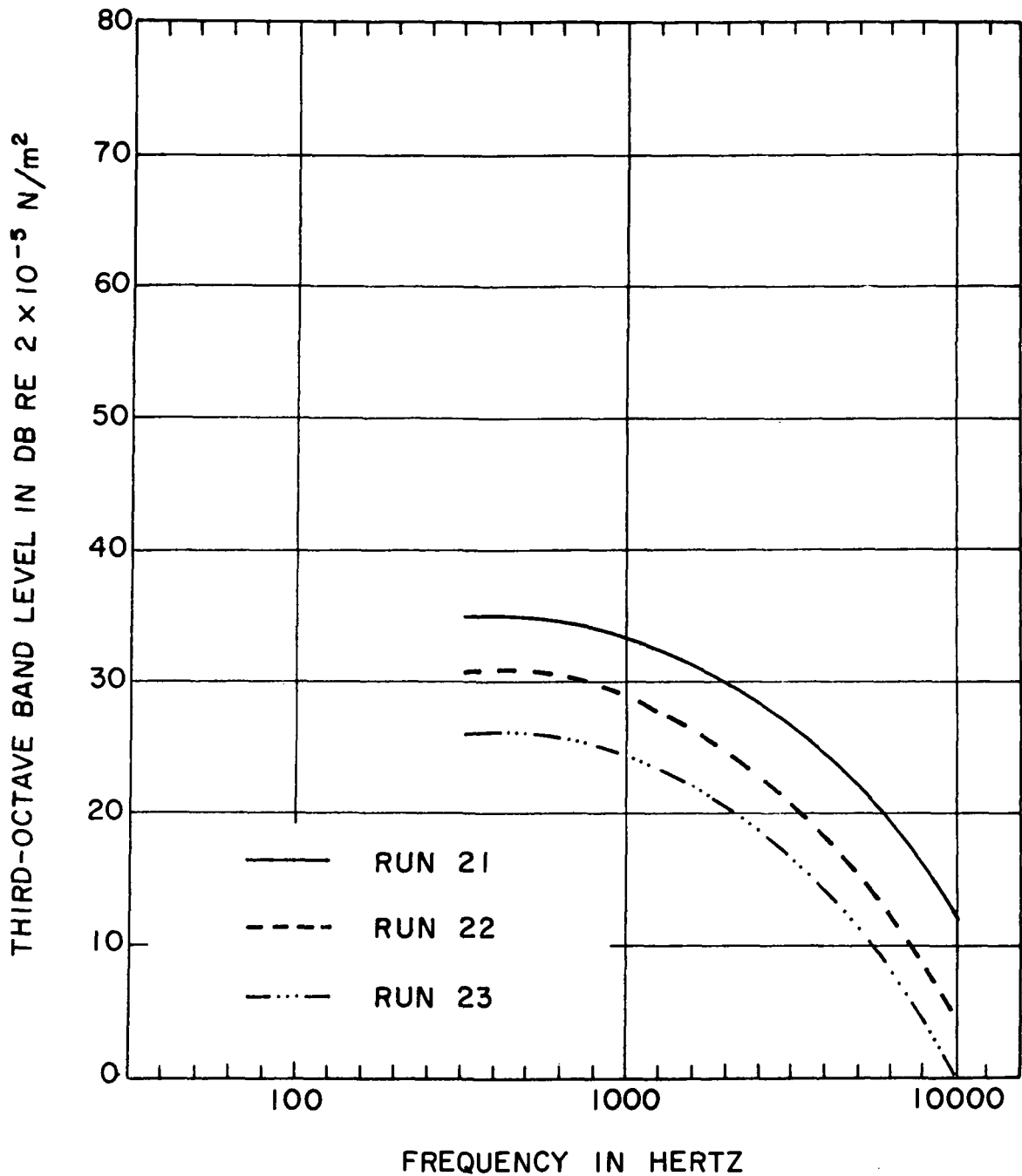
Figure 20(A). – Prue-2 (Glider) Idealized Noise Spectra – Light Gross Weight
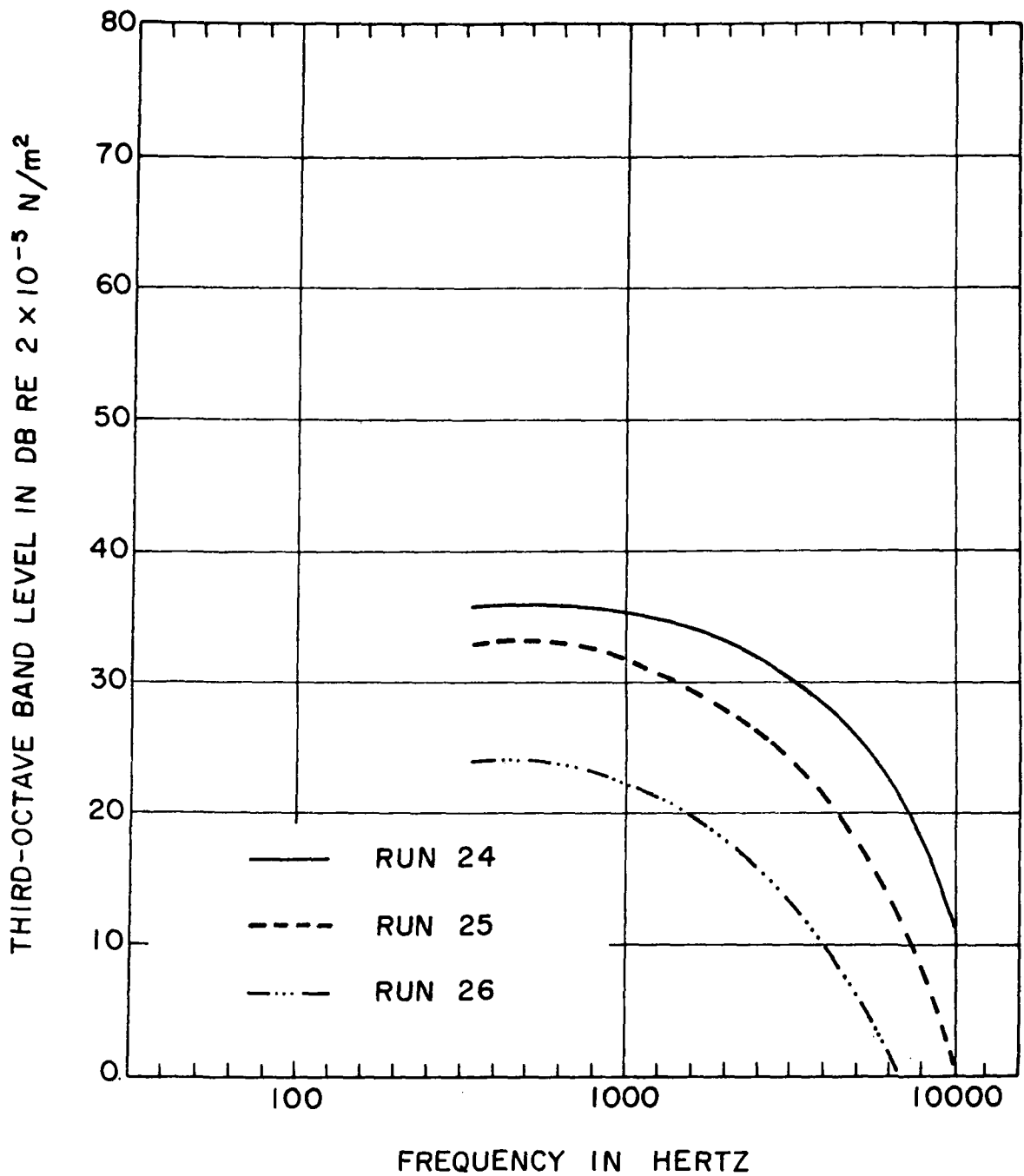
Figure 20(B). – Prue-2 (Glider) Idealized Noise Spectra – Heavy Gross Weight
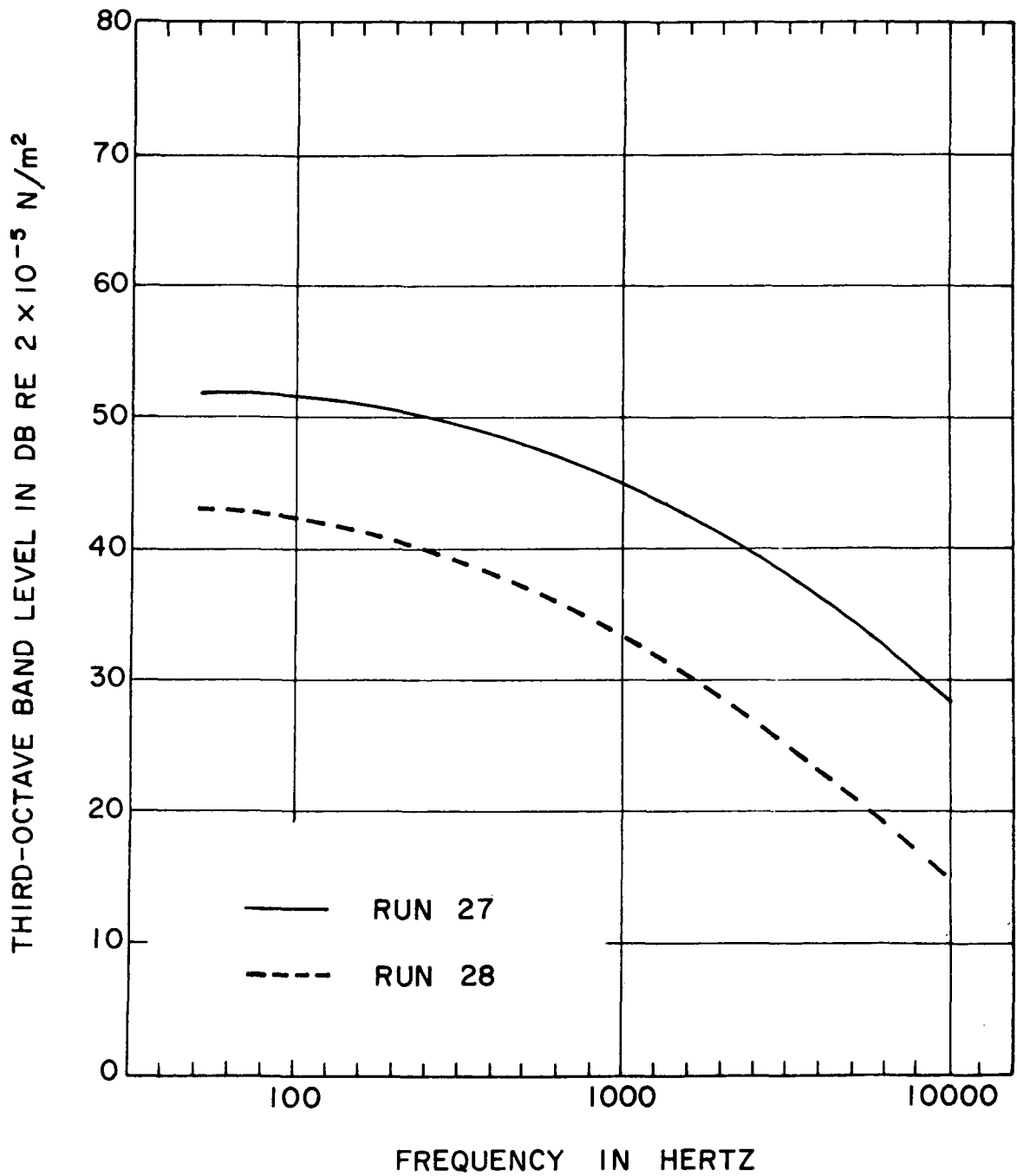
Figure 21. - Cessna 150 Idealized Noise Spectra

TABLE III

OVERALL SOUND PRESSURE LEVEL COMPARISON AT 152.4 METERS ALTITUDE

Aircraft	Test Run No. (n)	Velocity		Overall Sound Pressure Level, dB	
		m/sec	knots	Composite (Actual) Spectra	Idealized ("Smoothed") Spectra
Convair 240	1*	98.52	191.5	82.9	80.5
	2*	90.18	175.3	82.7	79.1
	3*	82.0	159.4	80.5	77.0
	4*	75.11	146.0	79.2	75.4
	5**	97.08	188.7	82.7	80.5
	6**	85.71	166.6	82.2	77.1
	7**	77.84	151.3	79.3	73.8
Douglas DC-3	8*	76.29	148.3	78.5	77.0
	9*	65.18	126.7	74.8	72.8
	10*	55.41	107.7	71.4	68.7
	11**	75.88	147.5	79.6	78.4
	12**	66.88	130.0	76.1	74.5
	13**	55.77	108.4	72.3	69.1
Aero-Commander Shrike	14*	89.72	174.4	75.4	74.5
	15*	78.71	153.0	72.3	70.7
	16*	69.45	135.0	71.4	66.7
	17*	58.60	113.9	70.2	61.3
	18**	81.59	158.6	73.1	70.9
	19**	70.58	137.2	72.7	68.3
	20**	62.40	121.3	68.9	64.9
Prue-2 (Glider)	21*	51.34	99.8	57.5	46.6
	22*	42.08	81.8	48.4	42.3
	23*	32.77	63.7	48.2	37.4
	24**	51.39	99.9	59.5	48.3
	25**	42.13	81.9	50.5	44.6
	26**	30.40	59.1	55.9	35.3
Cessna 150	27*	46.66	90.7	66.5	61.8
	28*	29.89	58.1	53.8	52.0

* Light gross weight } see Table I
** Heavy gross weight }

Exponent Evaluation

The exponents of equation 2, or the "X" coefficients for the logarithm terms of equation 3, were analyzed by two different methods. The first method was graphical in nature while the second, a regression analysis, was entirely statistical.

Two conditions are necessary in order to perform the graphical exponent evaluation: (1) the parameters must act independently and (2) only the parameter being evaluated should be allowed to vary -- all others being held constant. In actuality this cannot be done; however, if one parameter has a higher exponent than the others, its influence on the OASPL will be stronger than that of the other parameters, thereby permitting evaluation of that exponent. This was shown to be the case for the velocity where the basic data follow a V^6 relationship (figure 16). After each exponent was evaluated the OASPLs were then "normalized" by adjusting the different measured OASPL values to one common value of the parameter evaluated. In the case of the velocity the data were normalized to 61.2 meters per second (120 knots), a velocity within the operational range of a number of the measured aircraft. This process was repeated until all influential parameter exponents were evaluated. The procedure for graphical evaluation involves plotting the OASPL on a linear scale with the parameter under evaluation being plotted on a logarithmic scale. The slope of the line through the data values determines the value of the exponent. The data scatter was such that it was possible to place these lines in a manner to give slopes of integer values, thereby constraining the exponents to integer quantities.

In analyzing the data measured in the original program the influence of velocity was considered first, as mentioned above. Of the remaining parameters, the aspect ratio (AR) exhibited the strongest effect, having an exponent value of minus four ($X7 = -4$). The data, when plotted against aspect ratio, also had the least scatter compared to the other parameters. The OASPLs were then normalized to an AR = 10 and replotted against each of the remaining parameters. The results showed that the wing area (S) had the least data scatter among the remaining parameters, and hence best correlation with the measured data; the exponent was plus one ($X2 = +1$). Again the OASPLs were normalized, this time to a value of $S = 37.2 \ m^2$ (400 ft^2), and the results plotted for each of the remaining parameters. All of the remaining exponents showed a zero value, thereby concluding the graphical exponent evaluation.

The statistical analysis used for these data was based on equation 3. This approach resulted in a linear type of regression analysis employing a least square fit. Two sets of regression analyses were carried out on these data. The first set did not constrain any of the parameters, including the velocity. This set verified the results of the graphical analysis by yielding approximately the sixth power of velocity, the first power of wing area, and the negative fourth power of aspect ratio. The analysis, however, produces non-integer exponents; consequently, a second set of regression analyses was carried out with the velocity constrained to the sixth power. While the results from this set agreed with those from the first set, the correlation coefficient was higher and the standard error of estimation was lower. In carrying out both sets of analyses it was found necessary to exclude redundant parameter groups, such as W and W/S; W and W/b; S, C and b; etc., in order to obtain reasonable results.

This concluded the exponent evaluation.

Resulting Equation

The results of the foregoing exponent evaluation are summarized in the following equation:

$$OASPL = 10 \log_{10} \left[\left(\frac{\sin \phi}{r} \right)^2 \left(\frac{M^6 S}{AR^4} \right) \right] + constant \tag{4}$$

Determination of the constant was carried out in two steps; the first compared the calculated OASPLs for each of the 28 test cases with the OASPL associated with the idealized frequency spectra, while the second compared the "raw" or actual measured OASPLs for the 20 two-engine aircraft test cases. Only the two-engine aircraft OASPLs were used from the measured data due primarily to the ambient noise problems and strong discrete tones that dominated the glider OASPL data. The constant was taken as the average of the differences between the calculated and measured levels for both the idealized and actual data. The results are presented in equations 5a and 5b for the idealized and actual data, respectively:

$$OASPL = 10 \log_{10} \left[\left(\frac{\sin \phi}{r} \right)^2 \left(\frac{M^6 S}{AR^4} \right) \right] + 178.4 \tag{5a}$$

$$OASPL = 10 \log_{10} \left[\left(\frac{\sin \phi}{r} \right)^2 \left(\frac{M^6 S}{AR^4} \right) \right] + 181.4 \tag{5b}$$

The Mach number was corrected to a temperature of 288°K (59°F). The angle ϕ, to a first order approximation, is the angle between the aircraft flight path and the line from aircraft to the observer for an observer on or near the projection of the flight path on the ground. Determination of the sideline radiation pattern for this noise was beyond the scope of the measurement program.

The constant in the generalized equation was also evaluated using the actual flight velocities uncorrected for temperature. These results for the idealized and actual data are presented in equations 6a and 6b, respectively:

$$OASPL = 10 \log_{10} \left[\left(\frac{\sin \phi}{r} \right)^2 \left(\frac{V^6 S}{AR^4} \right) \right] + 26.4 \tag{6a}$$

$$OASPL = 10 \log_{10} \left[\left(\frac{\sin \phi}{r} \right)^2 \left(\frac{V^6 S}{AR^4} \right) \right] + 29.5 \tag{6b}$$

For convenience, a single equation, defined as the geometric mean of the equations for the idealized and actual data, may prove to be the most useful since it would represent the far-field aerodynamic noise radiated from a "fairly clean" airframe. This is, perhaps, more representative of current transport aircraft since they are aerodynamically "cleaner" than the two-engine aircraft used in the test program. The equation, in terms of Mach number is:

$$OASPL = 10 \log_{10} \left[\left(\frac{\sin \phi}{r} \right)^2 \left(\frac{M^6 S}{AR^4} \right) \right] + 179.9 \tag{7}$$

and in terms of actual flight velocity is:

$$OASPL = 10 \log_{10} \left[\left(\frac{\sin \phi}{r} \right)^2 \left(\frac{V^6 S}{AR^4} \right) \right] + 28.0 \tag{8}$$

were SI units (ref. 12) are used throughout.

There are a number of possible variations of these basic equations. Several such variations are presented in Appendix B along with a table of constants for using other forms of units including "inconsistent" units.

Appendix C presents a list of conversion factors for converting from the English system of units to the SI units as a convenience to the reader.

Comparison with Measurements

The proof of any equation is how well the measured data from each of the individual test cases agree with the corresponding predicted values. Figures 22 and 23 present the results for both the idealized and actual data, respectively. It is readily evident by examining these figures that the correlation is particularly good for the idealized data, as expected, and still very acceptable for the majority of the actual data cases. As previously discussed, the ambient noise encountered during the glider test presented serious problems by dominating many of the OASPL values. This is evident by the relatively poor correlation for several of the glider cases (figure 23).

The idealized data exhibited a deviation of from +2.2 to -2.8 dB with respect to the corresponding calculated values while the actual data for the 20 two-engine aircraft cases had deviation values of +3.0 to -2.9 dB. The average deviations were ± 1 dB for the idealized data and +0.9 to -1.5 dB for the two-engine aircraft actual data.

Recently, aerodynamic noise tests have been conducted by the Lockheed-Georgia Company on a C-5A airplane (refs. 3 and 4). Appendix D details the comparison of one test case idealized spectrum prediction using the above developed method. Briefly, the portion of the measured spectrum attributed to aerodynamic noise gave an OASPL value
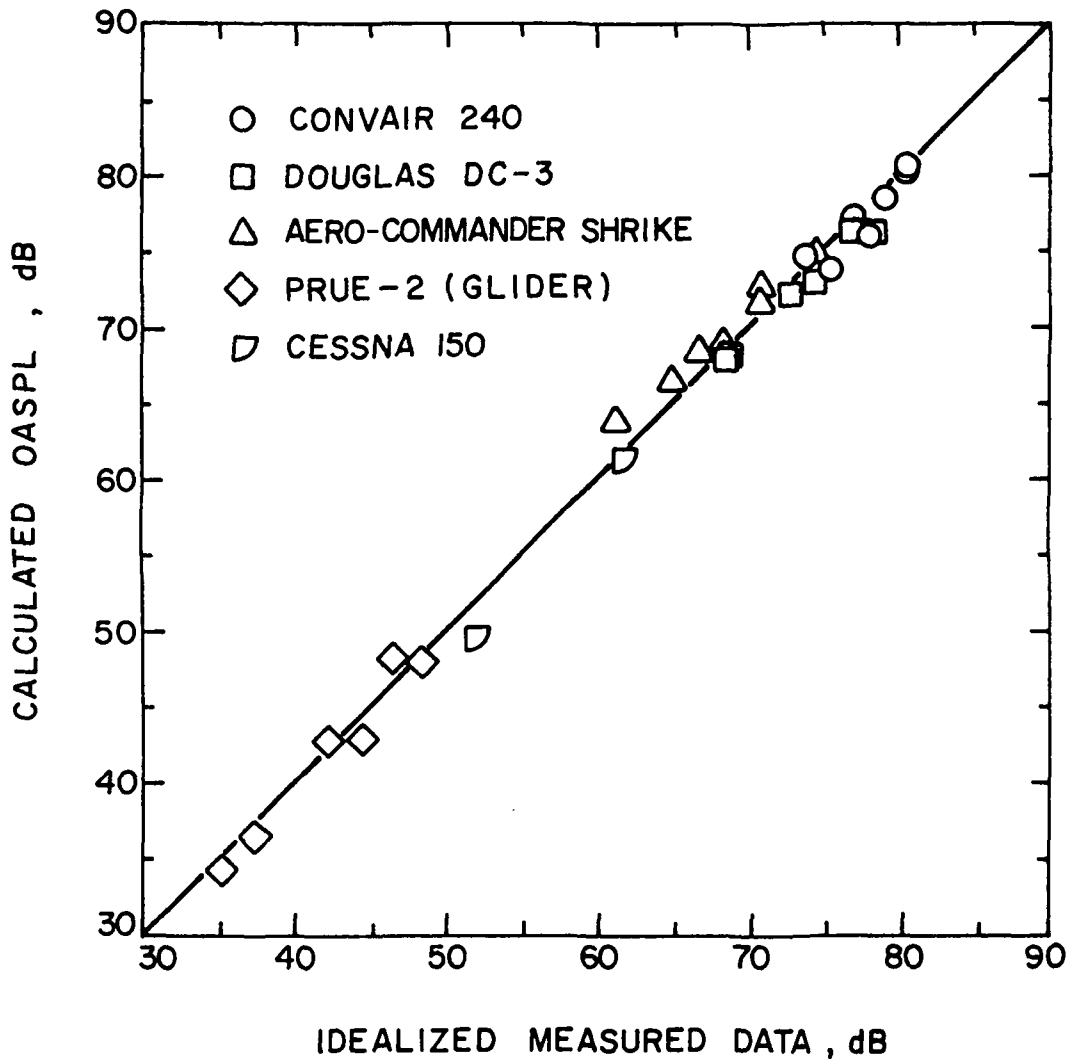
Figure 22. – Comparison of Idealized and Calculated Data
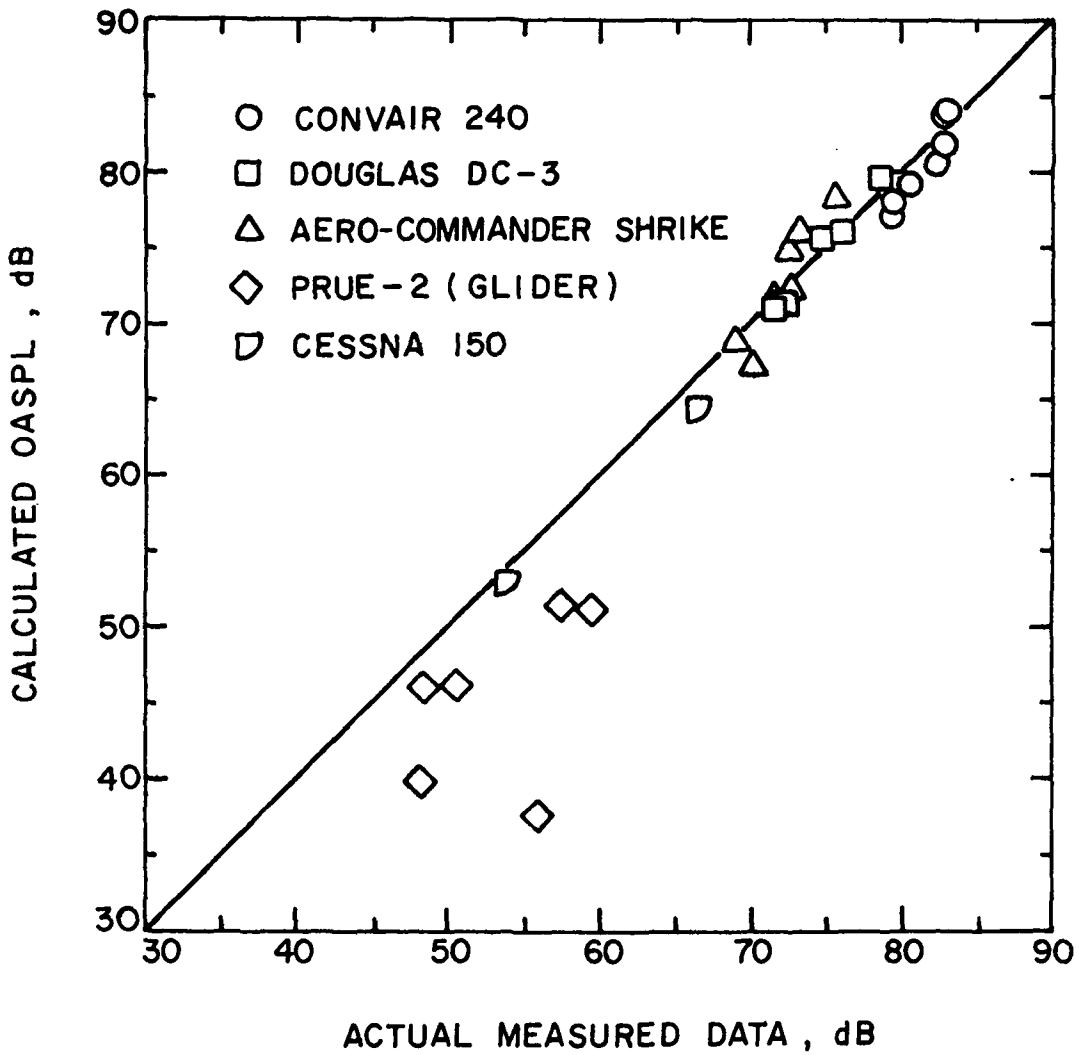
Figure 23. – Comparison of Measured and Calculated Data

of 100 dB while the corresponding calculated value was 99.3 dB. These results extend the range of the analysis to aircraft having gross weights that vary from 5785N (1300 pounds) to 2 713 415N (610 000 pounds) and for wing areas that vary from 14.6 sq m (157 sq ft) to 576 sq m (6200 sq ft); or a gross weight ratio of 470:1 and a wing area ratio of 40:1.

Frequency Spectral Analysis

In addition to predicting the magnitude of the far-field aerodynamic noise, it is also necessary to determine where, within the audible range of frequencies, this energy is produced. A conventional approach was taken for this analysis -- the use of a non-dimensional frequency spectrum that relates the peak frequency (f_{max}) to velocity (V) and a characteristic dimension (t) through a constant, the Strouhal number (S_t), as follows:

$$f_{max} = (S_t)\left(\frac{V}{t}\right) \tag{9}$$

The wing has been shown to be the dominant source of far-field aerodynamic noise for "clean" configured aircraft; consequently, the wing thickness (t) was used as the characteristic dimension. The frequency analysis involved determination of the most representative wing thickness - since wings vary in thickness from the root to the tip - that would produce the least scatter in Strouhal number. This analysis is complicated by the fact that the idealized frequency spectra exhibit a moderately broad peak, making the selection of f_{max} somewhat arbitrary. Only the spectra from the two engine aircraft were used in this analysis because they showed the most clearly defined peaked spectra.

Three different wing thicknesses were used in determining the appropriate Strouhal number. The first thickness (t_1) was taken at the point where the exposed area of one wing was divided in half; the second thickness (t_2) was taken at the point where the chord associated with t_2 equaled the exposed area of one wing divided by the exposed span of that wing; the third thickness (t_3) was similar to t_2 except that the actual ("aerodynamic") wing area and actual span were used.

It is noteworthy that the wing area given for an aircraft also includes part or all of that segment of the fuselage planform area determined by extension of the wing planform to the aircraft centerline. The reason for this is based on the fact that that segment of the fuselage actually contributes to the total lift of the wing. A typical spanwise plot of wing section lift would show only a slight dip across the fuselage, indicating that the fuselage, in that region, is producing lift.

The results of this analysis are presented in Table IV and show that both t_2 and t_3 provide the least scatter in S_t, with t_3 being slightly better than t_2; additionally, t_3 is the easiest to calculate. In calculating the S_t values for each test case it became apparent that the values associated with the heavy gross weight flights of the Aero-Commander Shrike (n = 18, 19, 20) were consistently lower than for the other test cases,

TABLE IV
STROUHAL NUMBER COMPARISON

Test Case No. (n)*	Strouhal Number for		
	t_1**	t_2**	t_3**
1	1.23	1.10	1.17
2	1.35	1.20	1.27
3	1.32	1.17	1.24
4	1.44	1.28	1.36
5	1.17	1.04	1.10
6	1.26	1.12	1.19
7	1.39	1.23	1.31
8	1.61	1.28	1.34
9	1.88	1.50	1.57
10	1.77	1.41	1.48
11	1.61	1.29	1.35
12	1.83	1.46	1.53
13	2.02	1.61	1.69
14	1.32	1.13	1.20
15	1.47	1.26	1.33
16	1.51	1.30	1.37
17	1.43	1.23	1.30
18	0.81	0.70	0.73
19	0.94	0.80	0.85
20	0.84	0.72	0.76
Averages:			
n = 1 to 20	1.41	1.19	1.26
n = 1 to 17	1.51	1.27	1.34

* See Tables I and II for details on aircraft and test case numbers.

** See text for definitions of t_1, t_2, t_3.

including the same aircraft at light gross weight. It appears that these flights may have been made with some flap deployment which apparently caused an increase in the effective wing thickness, thereby lowering the peak frequency. Consequently, two average values of S_t are presented in Table IV for each "t" definition.

The recommended definition for f_{max} is:

$$f_{max} = 1.30 \frac{V}{t} \tag{10}$$

where $t = t_3$ and the associated S_t is taken as the average between the values of S_t for $n = 1$ to 20 and $n = 1$ to 17, viz. 1.26 and 1.34.

It is interesting to note that the aforementioned C-5A data (Appendix D) shows a Strouhal number of 1.07. This fact, combined with the data scatter shown in Table IV, indicates that the Strouhal relationship is perhaps too simplified for accurate prediction of the peak frequency associated with far-field aerodynamic noise; however, a more elaborate approach is beyond the scope of the present program due primarily to the limited nature of these data.

Calculation of $t = t_3$ is very straightforward. The wing chord (C_3) associated with t_3 is defined as:

$$C_3 = \frac{S}{b} = \frac{\text{wing area}}{\text{wing span}} \tag{11}$$

The value of t_3 is determined from the wing thickness-to-chord distribution which may be either a constant ratio or a function of spanwise location. If this information is unavailable then 11 percent is a suitable typical value for transport-type aircraft, or $t = (0.11\ S/b)$.

Non-Dimensional Spectra

Having established methods for predicting both the magnitude and peak frequency of the far-field aerodynamic noise, there remains to be delineated the distribution of this energy throughout the audible frequency spectrum. This was accomplished by first non-dimensionalizing the frequency spectrum, i.e., dividing the actual frequency by the peak frequency, for each of the 20 two-engine test cases and then normalizing the magnitude by subtracting the corresponding OASPL value from each one-third octave band level for each of the test cases used. The result, expressed in terms of one-third octave band level relative to the OASPL and non-dimensional frequency, is presented in figure 24 along with the boundaries containing the majority of these data. This approach presupposes that both the OASPL and the peak frequency (f_{max}) of each test case used are equal to that calculated from the previously developed expressions.
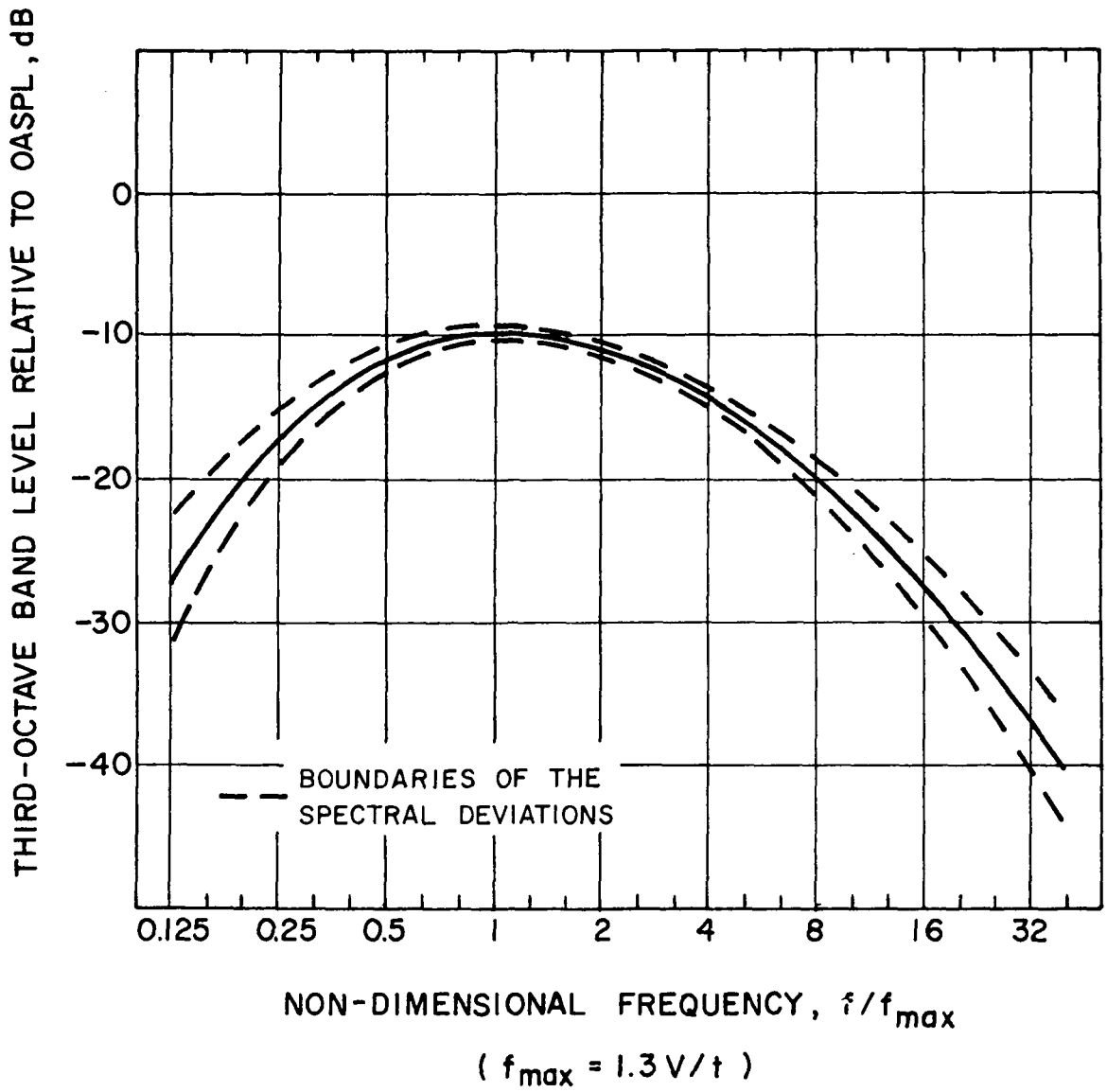
Figure 24. – Non-Dimensional Aerodynamic Noise Spectrum

To obtain the actual one-third octave band spectrum for an aircraft, the following procedure is recommended:

- calculate the value of f_{max} using equations 10 and 11 and the wing thickness-to-chord ratio,

- select the standard one-third octave band center frequency nearest the calculated value for f_{max},

- multiply the non-dimensional frequency scale of figure 24 by the above selected standard one-third octave band center frequency for f_{max} to obtain an absolute one-third octave band frequency scale,

- calculate the associated OASPL value using either equation 5, 6, 7, or 8,

- add the calculated OASPL value to the relative one-third octave band level scale shown in figure 24 to obtain an absolute level scale in dB.

Once this is completed, it is then necessary to incorporate the effects of atmospheric absorption into the applicable one-third octave bands. This is to be done in accordance with the procedure of reference 10, remembering that the reference distance is 152.4 meters (500 feet).

CONCLUSIONS

This initiatory systematic investigation of far-field radiated aerodynamically generated noise encompassed a broad spectrum of aircraft. Flyover noise measurements were conducted for five gliding aircraft with gross weights which ranged from 5785 to 173 925N (1300 to 39 000 lb), flyover velocities from 30 to 98.5 m/sec (58 to 191.5 knots or 98 to 323 ft/sec) and wing aspect ratios from 6.59 to 18.25.

Based on these noise measurements, a theory-based empirical relationship was developed which showed the important parameters for the prediction of the aerodynamic noise OASPL to be velocity (Mach number), wing area, and aspect ratio in addition to the normal distance factor. The equation is given by the simple expression:

$$\left.\begin{array}{l}\text{Overall}\\\text{Radiated}\\\text{Noise (dB)}\end{array}\right\} = 10\log_{10}\left[\frac{(\text{Mach No.})^6\ (\text{Wing Area})}{(\text{Distance})^2\ (\text{Aspect Ratio})^4}\right] + \text{constant}$$

This relationship, developed from an idealized form of the measured spectral data, was found to have maximum deviations, for the idealized data, of +2.2 to -2.8 dB with an average deviation of ±1 dB. When compared to the measured data for the two-engine aircraft the maximum deviations were +3.0 to -2.9 dB with average deviations of +0.9 to -1.5 dB.

Another relationship was also developed for calculating the peak frequency of the broadband aerodynamic noise. This expression uses the vehicle velocity, mean wing thickness, and a Strouhal number developed from the idealized measured spectral data. A non-dimensional frequency spectrum was then developed which makes possible the calculation of the one-third octave band frequency spectrum associated with this noise source.

Using the relationships developed herein, it is now possible to predict, with a reasonably high level of confidence, both the magnitude and frequency distribution of the far-field radiated aerodynamically generated noise from "clean" configured aircraft. This noise level represents the absolute minimum noise that an aircraft in flight can be expected to produce, or the noise "floor." Knowledge of this minimum aircraft noise level sets the limits for effective powerplant noise reduction. Also, governmental regulatory agencies now have a method for determining minimum practical noise limits for transport aircraft. In addition, these relationships give the aircraft designer some convenient guidelines for optimizing the design of an aircraft for minimum aerodynamic noise.

One of the primary constraints of this program was that of flying the aircraft in only an aerodynamically "clean" configuration, viz. no flaps, wheels up, etc. It appears obvious, and recent tests (refs. 2, 3, and 4) confirm the assumption, that any deviation from a "clean" configuration will generate additional noise at different frequencies. This limitation of the present study should be kept in mind when performing aerodynamic noise predictions using the method presented herein.

APPENDIX A

TABULATION OF ONE-THIRD OCTAVE BAND DATA

The data presented in the following two tables (Tables A-IA and A-IB) are the maximum one-third octave band levels attained during the associated flyover corrected to an altitude of 152.4 meters (500 feet). The correction to a constant altitude involved the application of both spherical spreading and atmospheric absorption effects. In the case of the Prue-2 glider data, corrections were also applied for the ambient noise by the method of energy subtraction. Several of the glider data band levels fell below the corresponding band levels of the measured ambient noise, erroneously indicating the absence of data. This is due to the low frequency variability of the ambient noise. In these cases the band levels were obtained by linear interpolation between the adjacent bands, and are denoted by parenthesis in the tabulation.

TABLE A-IA
MEASURED MAXIMUM ONE-THIRD OCTAVE BAND SOUND PRESSURE LEVELS AT 152.4 METERS ALTITUDE

1/3 OB FREQ Hz	CONVAIR 240							DOUGLAS DC-3					
50	65.1	69.0	68.8	69.0	65.3	68.2	66.3	63.2	60.9	59.2	65.3	61.8	58.6
63	64.7	66.0	66.0	64.4	66.8	66.9	63.9	65.1	59.8	60.2	65.4	59.8	61.8
80	68.2	70.5	71.1	66.3	70.3	71.7	70.4	61.7	58.4	56.6	65.2	61.2	57.3
100	74.4	75.1	73.0	70.1	73.8	74.9	72.4	68.0	64.6	61.3	69.4	67.4	62.5
125	76.5	76.2	73.9	73.3	76.6	76.4	73.1	70.6	67.4	64.4	71.6	69.2	65.5
160	74.1	74.3	71.1	71.0	74.5	74.1	70.0	69.8	64.8	62.6	70.9	66.9	63.3
200	71.5	70.1	67.6	66.7	71.6	69.8	66.7	67.3	62.7	61.9	68.3	62.9	60.4
250	71.5	70.1	66.9	66.0	71.1	69.5	66.6	67.7	65.0	59.2	69.0	66.0	61.6
315	69.6	69.7	66.4	65.2	69.7	67.1	64.5	67.2	63.7	58.9	68.1	64.0	59.3
400	69.1	68.1	66.0	64.6	69.2	66.0	62.9	66.6	62.2	57.5	67.8	64.2	59.4
500	69.5	67.8	64.9	63.1	68.5	66.6	62.8	65.3	62.2	57.0	66.8	63.4	58.2
630	68.8	67.5	63.9	62.8	67.9	64.8	61.4	65.4	61.9	56.2	66.2	62.6	57.4
800	67.4	66.2	62.9	61.6	66.2	63.2	59.7	64.3	60.6	55.5	65.0	61.3	56.6
1000	66.9	65.4	61.9	60.7	64.8	61.3	57.4	62.4	59.1	53.3	63.6	59.4	54.9
1250	66.1	64.2	61.2	60.1	63.0	59.6	56.5	61.0	57.7	52.8	62.2	58.3	53.4
1600	64.2	62.5	59.4	58.3	60.1	57.3	54.1	58.8	55.9	51.1	59.7	56.2	51.5
2000	61.8	60.7	57.1	56.5	57.0	53.8	50.4	56.6	53.7	49.4	56.6	53.3	50.6
2500	59.4	58.0	55.1	54.0	53.6	50.7	47.0	52.8	51.8	47.4	52.7	50.2	47.6
3150	56.3	55.6	53.7	55.5	50.7	48.1	46.7	52.7	49.5	42.8	51.3	48.0	41.9
4000	57.1	58.2	55.4	52.0	53.4	51.4	46.3	47.8	46.6	—	46.6	42.8	39.8
5000	54.0	52.6	46.6	—	49.1	43.8	—	42.0	40.8	—	40.9	36.7	34.5
6300	46.4	44.8	—	—	44.9	—	—	—	—	—	—	—	—
8000	39.6	46.7	—	—	45.2	—	—	—	—	—	—	—	—
10 000	32.6	46.7	—	—	44.8	—	—	—	—	—	—	—	—
OASPL	82.9	82.7	80.5	79.2	82.7	82.2	79.3	78.5	74.8	71.4	79.6	76.1	72.3
TEST RUN NO. (n)	1	2	3	4	5	6	7	8	9	10	11	12	13

Note: See Tables I and II for aircraft and test case information.

TABLE A-1B

MEASURED MAXIMUM ONE-THIRD OCTAVE BAND SOUND PRESSURE LEVELS AT 152.4 METERS ALTITUDE

1/3 OB FREQ Hz	AERO-COMMANDER SHRIKE							PRUE-2 (GLIDER)						CESSNA 150	
50	50.0	50.4	55.5	53.8	50.3	51.6	55.4	36.3	40.5	42.6	39.4	46.3	46.7	57.9	48.3
63	54.5	52.2	53.5	54.3	55.6	52.1	55.6	34.2	41.7	43.9	43.7	39.6	50.8	51.5	43.6
80	61.6	58.8	56.3	57.6	60.7	58.9	59.0	30.8	40.6	(39.5)	43.6	(40.2)	52.3	60.0	42.6
100	62.8	60.6	59.5	61.6	62.7	61.3	61.9	37.3	(39.0)	35.1	37.5	40.7	43.8	58.0	42.6
125	62.6	59.8	59.3	58.8	62.9	60.5	59.5	39.9	37.3	30.1	38.7	41.4	39.7	56.5	44.0
160	61.7	58.0	60.4	54.5	62.3	57.6	56.5	39.8	33.7	34.0	39.5	37.4	41.8	53.8	41.2
200	62.6	59.3	59.5	54.9	61.7	59.0	57.1	35.0	(33.6)	35.5	33.0	30.1	26.7	50.0	41.0
250	62.9	59.7	57.5	58.8	60.4	58.3	56.6	34.5	33.5	24.3	36.1	34.7	27.5	50.5	40.5
315	65.4	64.1	63.8	65.4	64.8	67.0	60.0	35.3	30.6	26.7	35.2	32.7	26.0	50.1	38.2
400	66.7	64.4	65.7	62.6	64.0	67.5	57.1	34.8	31.1	30.7	36.0	33.3	23.7	50.2	38.9
500	65.4	61.3	57.0	51.8	60.8	56.6	53.7	35.1	30.8	26.3	35.8	33.3	24.1	51.9	37.5
630	65.0	60.7	57.8	51.5	60.1	58.1	53.8	34.3	29.9	25.3	35.9	33.1	23.8	52.7	37.0
800	65.5	61.1	57.2	50.8	60.8	56.1	52.3	34.1	29.2	24.8	35.8	31.9	22.6	50.2	34.7
1000	63.1	59.1	54.8	49.2	58.5	54.5	50.2	44.6	32.6	23.2	45.7	31.4	21.6	52.3	39.6
1250	61.8	57.6	53.5	48.2	56.6	52.7	48.6	54.4	33.6	23.3	56.4	32.0	21.6	52.3	42.4
1600	59.4	55.4	51.4	46.1	53.9	50.6	46.7	52.6	26.4	22.1	54.3	28.9	19.8	51.8	30.3
2000	56.2	53.0	48.3	43.0	50.5	48.5	43.1	37.6	27.8	20.9	43.0	29.8	19.2	45.3	28.2
2500	53.1	49.7	45.3	43.6	46.6	44.0	42.0	38.4	27.4	20.5	40.0	27.3	17.1	43.2	26.6
3150	50.5	49.3	46.1	39.6	45.3	43.1	39.9	35.8	20.9	12.9	35.9	23.7	11.1	40.8	24.9
4000	49.7	49.2	42.3	35.8	45.2	43.0	35.9	31.3	18.9	13.5	32.7	21.8	11.5	40.0	23.9
5000	45.7	41.8	37.4	—	40.3	36.4	30.9	29.8	17.0	14.1	28.9	19.2	6.5	38.7	22.5
6300	40.5	35.8	33.3	—	38.2	35.6	29.7	23.4	8.0	8.5	23.3	13.4	—	38.1	22.4
8000	36.6	32.7	31.1	—	36.5	34.7	30.0	16.8	—	—	17.4	—	—	32.3	23.4
10 000	34.8	30.7	29.8	—	35.3	—	26.8	12.3	—	—	—	—	—	22.3	20.9
OASPL	75.4	72.3	71.4	70.2	73.1	72.7	68.9	57.5	48.4	48.2	59.5	50.5	55.9	66.5	53.8
TEST RUN NO. (n)	14	15	16	17	18	19	20	21	22	23	24	25	26	27	28

Note: 1. See Tables I and II for aircraft and test case information.

2. Numbers in ( ) are determined by a linear interpolation between the adjacent band levels.

58

APPENDIX B

VARIATIONS ON A THEME OF AERODYNAMIC NOISE

The equations developed herein for predicting the level of the far-field aerodynamic noise can also be expressed in other forms. One such form, somewhat more suitable to aircraft design work, incorporates the terms for the coefficient of lift, C_L, and wing loading, W/S, in these equations. The results for both the idealized and actual data, respectively, are:

$$OASPL = 10 \log_{10} \left[\left(\frac{\sin \phi}{r} \right)^2 \left(\frac{1}{C_L} \right)^3 \left(\frac{W}{S} \right)^3 \left(\frac{S}{AR^4} \right) \right] + 32.8 \qquad (B1a)$$

$$OASPL = 10 \log_{10} \left[\left(\frac{\sin \phi}{r} \right)^2 \left(\frac{1}{C_L} \right)^3 \left(\frac{W}{S} \right)^3 \left(\frac{S}{AR^4} \right) \right] + 35.9 \qquad (B1b)$$

where the constant $(2/\rho)^3$ has been incorporated into the constant term. In the foregoing equation the terms C_L and W/S are expressed separately in order to emphasize their relative importance in the total expression.

Throughout this report SI units have been used. By rewriting equations 6 or 8 in the following generalized form

$$OASPL = 10 \log_{10} \left[\left(\frac{\sin \phi}{r} \right)^2 \left(\frac{V^6 S}{AR^4} \right) \right] + K \qquad (B2)$$

different units can be used with only a change in the value of K. The following table presents K values for different sets of units for both the idealized and actual data as well as the "mean" value for use with equation 8.

V	S	r	CONSTANT (K)		
			Idealized	Actual	"Mean"
knots	ft^2	ft	9.1	12.2	10.7
ft/sec	ft^2	ft	-4.5	-1.4	-3.0

It is interesting to note that the constant in equation 5 is unaffected by a change of units providing a consistent set of units is used since $S \div r^2$ is dimensionless.

APPENDIX C

CONVERSION FACTORS

The following table, based on reference 12, is presented for the convenience of the reader.

To Convert	To	Multiply By
dynes/sq cm	newtons/sq m	.1
feet	meters	.3048
feet/sec	meters/sec	.3048
knots	meters/sec	.51444444
pounds (force)	newtons	4.4482216
slugs/cu ft	kg/cu m	515.379
sq ft	sq m	.09290304

APPENDIX D

COMPARISON WITH RECENT DATA ON THE C-5A GALAXY

In January 1973 a series of flights with the C-5A Galaxy were made by the Lockheed-Georgia Company for the purpose of measuring far-field aerodynamic noise under a variety of aircraft configurations. These data are being prepared under a NASA contract for publication as a Contractor's Report (ref. 4). The flights were made with the engines operating at the flight idle setting. One of these flights was made with the aircraft in a "clean" configuration. The portion of the total vehicle noise spectrum attributed to the far-field aerodynamic noise was that below approximately 400 Hz. The measured data, adjusted to an altitude of 91.44 m (300 ft), are presented in the following table along with the corresponding idealized spectrum values. The idealized values, indicated by parentheses in the table, were obtained by extrapolating the drop-off between the 63 and 80 Hz bands to the 50 Hz band and the drop-off between the 160 and 200 Hz bands to the 250 315, and 400 Hz bands. The energy summation of these 10 third-octave bands is also presented.

Frequency (Hz)	Measured Data	Idealized Data
50	75	(68)
63	79	79
80	90	90
100	95	95
125	95	95
160	93	93
200	87	87
250	89	(81)
315	82	(75)
400	81	(69)
OASPL (50 - 400 Hz)	100.4	100.0

The corresponding test condition aircraft dimensional data are:

Gross weight: 2 713 415N (608 000 lb)

Wing area: 576 sq m (6200 sq ft)

Aspect ratio: 8.0

Altitude: 91.44 m (300 ft)

Velocity: 101.9 m/sec (198 knots)

The OASPL calculated by equation 8, considered more suitable for predicting the aerodynamic noise from current transport aircraft, is 100.9 dB while that calculated by equation 6a for the idealized spectrum is 99.3 dB. The remarkable accuracy of this sizeable extrapolation, 0.5 to 0.7 dB, verifies the essential validity of the analysis and permits such extrapolations with a reasonably high level of confidence.

REFERENCES

1. Gibson, J. S.: The Ultimate Noise Barrier. Proceedings of the Institute of Noise Control Engineering (Inter-Noise 72), October 1972, pp. 332-337.

2. Blumenthal, V. L.; et al.: Aircraft Environmental Problems. Paper 73-5, Am. Inst. Aeron. and Astronaut, January 1973.

3. Gibson, J. S.: Non-Engine Aerodynamic Noise: The Limit to Aircraft Noise Reduction. Paper F22Y12, Proceedings of the Institute of Noise Control Engineering (Inter-Noise 73), August 1973, pp. 445-454.

4. Gibson, J. S.: Non-Engine Aerodynamic Noise Investigation Of A Large Aircraft, NASA CR-2378, 1974 .

5. Gibbs, J. B.; and Healy, G. J.: Noise From A Gliding DC-3, Report LR 23328, Lockheed-California Company, March 15, 1970.

6. Brooks, P. W.: The World's Airliners, Putnam and Company (London), 1962, pp. 143-149; 211-217.

7. Anon.: Sales Brochure 1969, Aero-Commander Division, North American Rockwell Company.

8. Anon.: The World's Sailplanes. OSTIV and Swiss Aero Review, Regina-Druck (Zurich, Switzerland).

9. Anon.: Owners Manual 1967. Cessna Corporation.

10. Anon.: Standard Values of Atmospheric Absorption as a Function of Temperature and Humidity for Use in Evaluating Aircraft Flyover Noise, Society of Automotive Engineers, ARP-866, 1964.

11. Morse, P. M.; and Ingard, K. U.: Theoretical Acoustics, McGraw-Hill Book Company, Inc., 1968, pg. 762.

12. Mechtly, E. A.: The International System of Units, NASA SP-7012, 1973.

"The aeronautical and space activities of the United States shall be conducted so as to contribute . . . to the expansion of human knowledge of phenomena in the atmosphere and space. The Administration shall provide for the widest practicable and appropriate dissemination of information concerning its activities and the results thereof."
—NATIONAL AERONAUTICS AND SPACE ACT OF 1958

NASA SCIENTIFIC AND TECHNICAL PUBLICATIONS

TECHNICAL REPORTS: Scientific and technical information considered important, complete, and a lasting contribution to existing knowledge.

TECHNICAL NOTES: Information less broad in scope but nevertheless of importance as a contribution to existing knowledge.

TECHNICAL MEMORANDUMS: Information receiving limited distribution because of preliminary data, security classification, or other reasons. Also includes conference proceedings with either limited or unlimited distribution.

CONTRACTOR REPORTS: Scientific and technical information generated under a NASA contract or grant and considered an important contribution to existing knowledge.

TECHNICAL TRANSLATIONS: Information published in a foreign language considered to merit NASA distribution in English.

SPECIAL PUBLICATIONS: Information derived from or of value to NASA activities. Publications include final reports of major projects, monographs, data compilations, handbooks, sourcebooks, and special bibliographies.

TECHNOLOGY UTILIZATION PUBLICATIONS: Information on technology used by NASA that may be of particular interest in commercial and other non-aerospace applications. Publications include Tech Briefs, Technology Utilization Reports and Technology Surveys.

Details on the availability of these publications may be obtained from:

SCIENTIFIC AND TECHNICAL INFORMATION OFFICE

NATIONAL AERONAUTICS AND SPACE ADMINISTRATION
Washington, D.C. 20546